中国激光

异质金属激光增材制造研究及应用进展(特邀)

马毅[1], 管迎春[1,2*]

[1]北京航空航天大学机械工程与自动化学院, 北京 100083;

[2]北京航空航天大学大型金属构件增材制造国家工程实验室, 北京 100191

摘要 极端服役环境对空天等核心构件可靠性和集成性提出了严峻挑战。传统单一材料体系和制造工艺难以满足复杂性能需求。激光增材制造技术是实现异质金属结构-功能一体化的有效途径,但异质材料兼容问题(易诱发缺陷、加工参数响应不一等)限制了高质量异质界面的形成,这对制造装备与连接工艺提出了更高挑战。本文基于异质金属激光增材制造的最新研究进展,聚焦异质金属成型的关键问题及解决方案,回顾了近年来异质金属体系的发展及空天领域应用,从送粉方式、复合制造等方面介绍了激光增材装备的改进策略,总结了近年来激光增材技术在连接方式、参数调控、监测预测和前后端处理方面的研究进展,并针对这一技术的共性及难点问题给出了展望与思考。

关键词 激光技术; 异质金属; 空天应用; 增材装备; 增材制造工艺

中图分类号 TN249 **文献标志码** A **DOI**: 10.3788/CJL240428

1 引 言

近年来,异质金属构件因其优异的机械和物化性能引起了广泛关注[1-2]。利用异质金属间的优势互补关系,构建出性能梯度或功能材料界面,可实现特定应用场景目标性能的精准定制。尤其在航空航天领域,异质金属不仅能够提供轻量化设计和热管理,还能在强度与耐蚀性等方面实现综合优化,为各种极端服役环境下的构件设计提供了全新的思路。无论是承力结构部件[3]或是发动机功能组件[4],均展现出对异质金属结构的高度需求。

传统异质金属制造方法,如粉末冶金、焊接、轧制、铸造等,虽然能够实现异质金属的连接,但难以满足复杂构件对于成型自由度和成分可控性的制造要求[5]。相较之下,增材制造技术通过其独特的层层堆叠制造方式,为异质金属的多样化连接提供了全新的解决途径。目前,异质金属增材制造的方法主要包括粉末床熔化和定向能量沉积技术,通过对不同热源(激光[6]、电弧[7]、电子束[8])的精准调控,可有效实现异质金属的一体化成型。

激光增材制造(LAM)技术由于其高成型精度和可控性,在异质金属增材制造中备受关注。LAM能够提供精准的能量控制和局部熔化,从而实现微观尺度上异质金属间的良好冶金结合。根据送粉方式的差异,LAM技术可进一步细分为激光粉末床熔化(LPBF)技术(通常也被称为选择性激光熔化SLM)和激光定向能量沉积(LDED)技术(通常也被称为激光金属沉积LMD或激光近净成形LENS)。其中,LPBF通过预制异种粉末层并逐层激光熔化,可以生产出具有高表面光洁度和精细几何结构的样件[9];LDED则一般利用激光将金属粉材或线材沉积在基材上,兼具高灵活性和高自由度[10]。然而传统的激光增材装备无法适配异质金属的制造,且材料间的固有兼容性问题和工艺参数匹配问题制约了这一技术的实际应用。

面向空天等领域对于轻量、高强异质金属材料的迫切需求,本文聚焦激光增材制造异质金属的材料体系、相关应用、装备水平和工艺优化,重点对该领域的国内外最新成果进行梳理和探讨,分析了该技术的瓶颈问题及相关的解决方案,并对这一领域未来的发展方向进行了展望。

2 异质金属材料体系及需求应用

2.1 异质金属体系研究现状

激光增材技术的快速发展拓宽了异质金属间的组合种类,并使得热物性差异悬殊的异质金属连接成为了可能。铜、镍、铁、钛和铝及其合金是目前激光增材制造的主要材料,通过不同体系组分优化设计和制造过程控制,将具有互补性能(机械性能、物化性能)的异质材料集成到一个构件中,进而满足空天、生物、核工业等不同应用场景下的需求。表1汇总了目前典型异

收稿日期: 2024-01-02; **修回日期**: 2024-01-28; **录用日期**: 2024-02-19; **网络首发日期**: 2024-02-29

基金项目: 宁波重点研发专项(2023Z012)

通信作者: *guanyingchun@buaa.edu.cn

质金属体系的组合、性能表现及潜在应用。其中，基于316L、Inconel 718、Ti6Al4V 合金和 Ni/Fe 组合的异质连接研究较为广泛，基于 W、Co 等大物性差异的异质连接也成为了可能。此外，探索新型异质金属体系，例如 Ta/Ti、Ag/Cu 等，是未来拓宽技术应用的重要发展方向。

表1 典型异质金属体系及其性能和应用

Table 1 Typical heterogeneous metal systems and their properties and applications

Material system	Material property	Application	Typical heterogeneous metal system
Cu/Ni	Thermal conductivity/heat resistance/high strength	Aerospace thrust components/integrated circuit	Inconel 718/GRCop84[11] NiTi/CuSn10[12] Inconel 718/ CuCr0.8[13]
Cu/Fe	High stiffness/electrical conductivity/thermal conductivity/wear resistance	Nuclear industry/power generation industry/automobile industry	316L/CuSn10[14] 316L/C52400[15] 316L/CuCrZr[16]
Cu/Ti	Heat resistance/high specific strength	Aerospace heat exchanger	Ti6Al4V/Cu[17] Ti6Al4V/CuNi2SiCr[18] Cu10Sn/Ti6Al4V[19]
Cu/Al	Electrical/thermal conductivity/low density	Energy conduction/cooling device/solar collector	AlSi10Mg/C18400[20]
Ni/Fe	High strength/corrosion resistance/oxidation resistance	Gas turbine/power generation equipment/heat exchanger	316 L/Inconel 718[21] 316L/Inconel 625[22] SS420/Inconel 718[23]
Ni/Ti	Biocompatibility/wear resistance/high specific strength/heat resistance	Aerospace thermal protection system/orthopedic implants	Inconel 718/Ti6Al4V[24] TC4/Inconel 625[25] NiTi/Ti6Al4V[26]
Fe/Ti	High specific strength/corrosion resistance	Aerospace engines/load-bearing components	Ti6Al4V/316L[27]
Fe/Al	High strength/corrosion resistance/lightweight	Automotive manufacturing/aerospace hydraulic systems/space launch systems	316L/AlSi10Mg[28] 316L/Al[29]
Ti/Al	Lightweight/ductility and malleability/high strength	Aerospace and automotive structural component	Ti6Al4V/AlSi10Mg[30] AA2024/Ti6Al4V[31] Ti6Al4V/Al12Si[32]
Co/Ti	Biocompatibility/high strength	Medical implant	CoCrMo/Ti6Al4V[33]
Co/Ni	Corrosion resistance/high strength	Nuclear industry/petrochemical industry	CoCrMo/Inconel 718[34] CoCrMo/Inconel 625[35]
Co/Fe	Heat resistance/wear resistance/high toughness	Machining tools and mold manufacturing	SS316L/CoCrMo[36]
W/Cu	Electrical/thermal conductivity/resistance to plasma radiation	Integrated circuit radiator/electrode/nuclear industry	Cu10Sn/W[37]
W/Fe	Ductility and malleability/resistance to plasma radiation/high strength	Nuclear industry	W/316L[38]

2.2 空天异质金属体系及应用

Cu/Ni 异质体系是空天领域应用最广泛的材料组合。Cu 及其合金具有出色的热导率和机械性能，而 Ni 及其合金则兼具优异的高温蠕变、抗氧化性能和强韧性。通过激光增材技术进行耦合，可以最大程度地发挥这两类材料的特性，以满足复杂的热梯度变化，确保组件在极端工况下的可靠性和稳定性。以美国国家航空航天局(NASA)为例，通过对材料体系和工艺的创新，成功制备了一系列高性能的异质金属耦合航天推力组件[39]。通过开发新型 GRCop-42(Cu-Cr-Nb)铜合金和 HR-1(Fe-Ni-Cr)高温合金，利用 LPBF 和 LDED 工艺制备功能梯度层，通过调控激光参数，进而实现两类材料的可靠键合[图 1(d)]。在此基础上，NASA 制造了集蠕变性能、高温强度、抗氧化、耐腐蚀性能于一身的高性能推力组件，包括火箭燃烧室[图 1(a)][39]、喷注器[图 1(b)][39]和耦合推力组件[图 1(c)][39]。此外，通过整合一些新技术，例如 LPBF+BP-DED(吹塑粉末定向能量沉积)，NASA 还设计出一些新型 Cu/Ni

双金属构件[40]，例如 GRCop-84 燃烧室[图 1(e)]和 Ni 基通道冷却喷嘴[图 1(f)]，并将这两类构件成功耦合[图 1(g)]。

DMG MORI 公司在这一领域实现了重要突破。他们不仅采用混合激光增材制造工艺(SLM+LDED)成功制备了尺寸为 500 mm×680 mm 的异质金属耦合火箭喷嘴组件[图 1(h)][41]，还通过 LDED 工艺制造了尺寸为 300 mm×250 mm 的火箭发动机组件[图 1(i)][41]。这些样件基于(C18150/CuNi2SiCr)/Inconel 625 的体系设计，证明了激光增材技术构建大型 Cu/Ni 航空构件的潜力。Fraunhofer IGCV 研究所也通过 SLM 成型了 Cu/Ni 双金属热交换器[图 1(j)][41]及火箭燃烧室缩比件[图 1(k)][42]，并有效提高了组件的整体耐热及热传导能力。

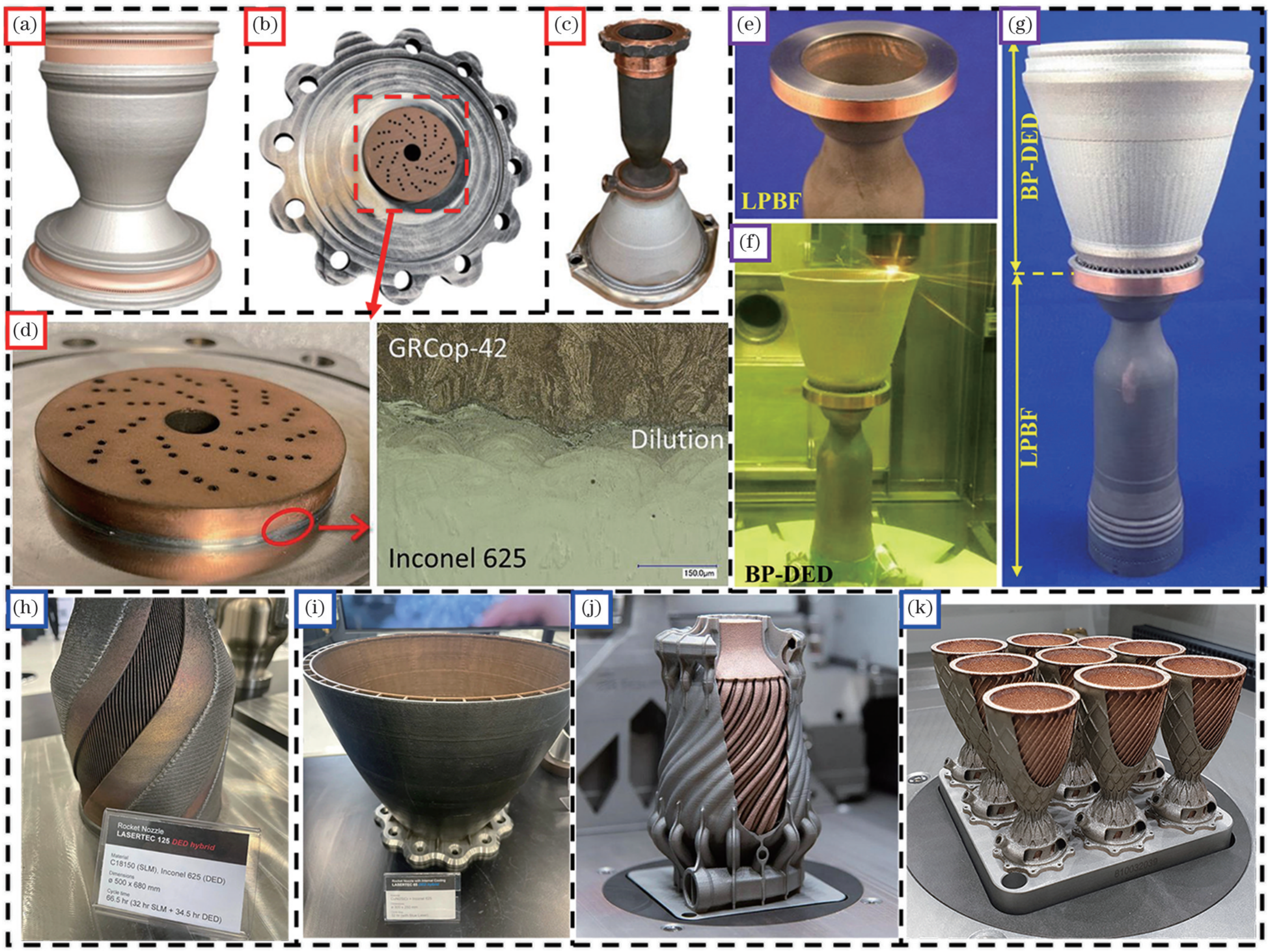

图 1　Cu/Ni 异质金属体系的空天应用。(a)LDED 工艺成型的 GRCop-42(Cu-Cr-Nb)/HR-1(Fe-Ni-Cr)燃烧室[39]；(b)LPBF 工艺成型的 Cu 基/Ni 基喷注器[39]；(c)LDED 工艺成型的耦合推力组件[39]；(d)喷注器结构及异质合金连接界面情况[39]；(e)LPBF 成型的 GRCop-42 燃烧室[40]；(f)BP-DED 工艺成型的镍基冷却喷嘴[40]；(g)耦合后的双金属结构[40]；(h)SLM+LDED 成型的 C18150/Inconel 625 火箭喷嘴[41]；(i)LDED 成型的 CuNi2SiCr/Inconel 625 火箭喷嘴[41]；(j)SLM 成型的 Cu 基/Ni 基双金属热交换器[41]；(k)SLM 成型的 Cu 基/Ni 基双金属燃烧室[42]

Fig. 1　Aerospace applications of Cu/Ni heterogeneous metal systems. (a) GRCop-42(Cu-Cr-Nb)/HR-1(Fe-Ni-Cr) combustion chamber formed by LDED[39]; (b) Cu-based/Ni-based injector formed by LPBF[39]; (c) coupled thrust assembly formed by LDED[39]; (d) injector structure and heterogeneous alloy connecting interface[39]; (e) GRCop-42 combustion chamber formed by LPBF[40]; (f) nickel-based cooling nozzle formed by BP-DED[40]; (g) coupled bimetallic structure[40]; (h) C18150/Inconel 625 rocket nozzle formed by SLM+LDED[41]; (i) CuNi2SiCr/Inconel 625 rocket nozzle formed by LDED[41]; (j) Cu-based/Ni-based bimetallic heat exchanger formed by SLM[41]; (k) Cu-based/Ni-based bimetallic combustion chamber formed by SLM[42]

Fe 及其合金(钢)因其高热稳定性、高耐蚀性，以及高成本效益而成为制造高性能空天支撑结构和功能部件的理想选择。当其与异质金属如 Cu、Ni、Al 耦合后，可以满足不同应用场景下的多性能需求。德国 Fraunhofer IGCV 和 MAN Energy Solutions SE 采用 LPBF 技术成功制造了 CW106C/1.2709 钢双金属大口径火箭发动机喷油嘴[图 2(a)][43]。这类设计显著提升了喷油嘴在服役过程中的耐高温能力，增强了高

应力区域的热传导效率，并优化了发动机的整体性能。2022年，InssTek公司采用LDED技术，制备了一款顶端由铝基青铜（高导热性）、底座由316L不锈钢（高强度）构成的火箭发动机喷嘴［图2（b）］[44]。这种设计适配了喷嘴不同部位在工作过程中的性能需求（底端和顶部的工作温度及热流差异明显），并通过中间的梯度过渡区有效避免了异质金属结合可能引起的断裂问题。2021年，Wits等[45]通过SLM技术将具有优异高温强度的镍基合金IN718与高低温延展性的SS316L钢连接起来［图2（c）］，制造出了一种航空航天双金属换热器。同年，Aerosint SA公司利用SLM技术成功制备出了尺寸为12.7 cm×7.3 cm×2.9 cm的CuCrZr/316L双金属管式换热器［图2（d）］[46]，兼具高热导率和高强度。

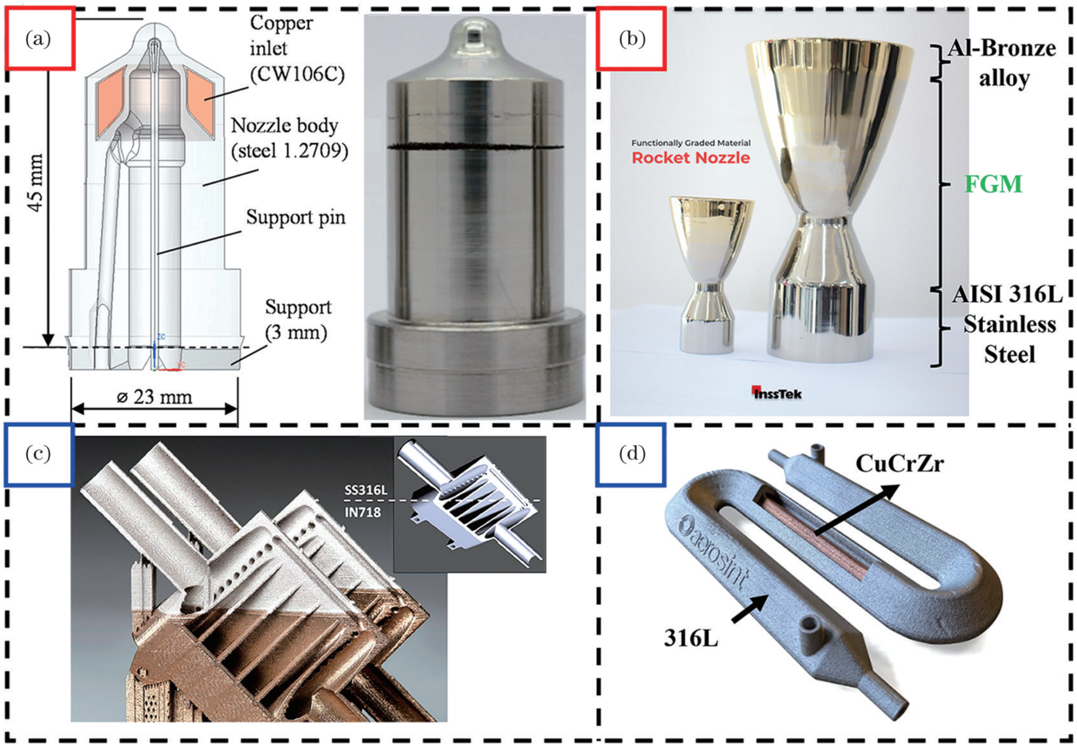

图2 Fe基异质金属体系的空天应用。(a)LPBF成型的CW106C/1.2709钢大口径发动机喷油嘴[43]；(b)LDED技术成型的316L/铝基青铜火箭发动机喷嘴[44]；(c)SLM成型的IN718/SS316L换热器[45]；(d)SLM成型的CuCrZr/316L换热器[46]

Fig. 2 Aerospace applications of Fe-based heterogeneous metal systems. (a) CW106C/1.2709 steel large caliber engine nozzle formed by LPBF[43]; (b) 316L/aluminum-based bronze rocket engine nozzle formed by LDED[44]; (c) IN718/SS316L heat exchanger formed by SLM[45]; (d) CuCrZr/316L heat exchanger formed by SLM[46]

钛及其合金具有高的比强度、耐蚀及耐高温性能，在与异质金属连接时，可以在保持轻量化的同时优化组件的综合性能。以Hofmann等[47]在2014年的工作［图3（a）］为例，他们设计并制造了一种

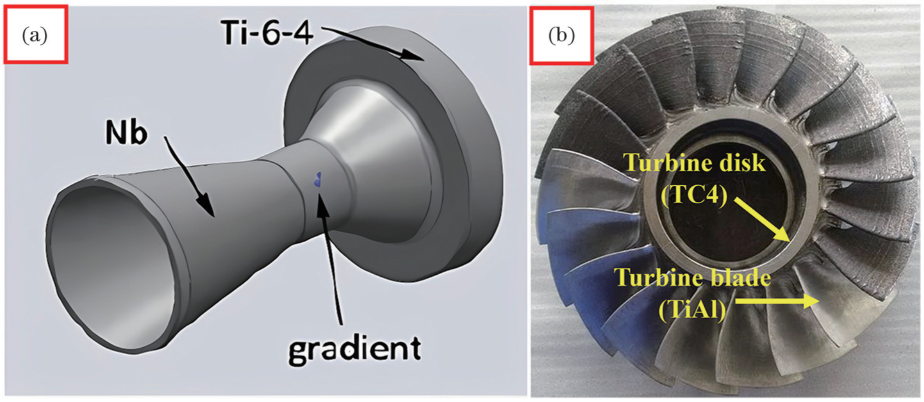

图3 Ti基异质金属体系的空天应用。(a)LDED技术成型的Ti6Al4V/Nb异质金属耦合火箭喷嘴组件[47]；(b)LDED成型的Ti6Al4V/Ti48Al2Cr2Nb涡轮叶片盘[48]

Fig. 3 Aerospace applications of Ti-based heterogeneous metal systems. (a) Ti6Al4V/Nb coupled rocket nozzle component formed by LDED[47]; (b) Ti6Al4V/Ti48Al2Cr2Nb turbine blade disk formed by LDED[48]

Ti6Al4V（轻质高强）和纯Nb（耐高温）的梯度火箭喷嘴原型。在这一组件中，耐高温的Nb构成了喷嘴部分，能够抵受高热负荷，而火箭主体则采用了Ti6Al4V，以降低整体密度。这种成分设计通过LDED工艺实现了无缝梯度过渡，保证了构件的可靠性。国内海博瑞思公司利用SVW80C-3D激光增减材混合设备，成功制造了Ti6Al4V/Ti48Al2Cr2Nb双金属结构［图3（b）］，适用于航空整体式涡轮叶片盘[48]。此外，Ti/Ni的梯度组件还可应用于航天热保护系统中，以减小连接部位因热梯度所引起的应力集中[49]。

3 异质金属激光增材装备现状

在传统激光增材制造过程中，设备通常被设计用于处理单一金属粉末的送粉和熔化。然而，随着异质金属增材概念的引入，对设备提出了更高的要求。异质金属增材不仅需要考虑不同金属粉末的送粉方式和混粉策略，还要考虑不同材料之间的物性差异。这些问题推动了现有激光增材装备的发展，以期实现精准控制多种材料的递送和沉积，同时确保材料间界面的结构完整性和性能一致性。表2列举了传统LAM装备在异质金属增材中的优劣势，并总结了可能的解决方案。

表2　传统LPBF及LDED技术在异质金属制造中的优势、局限性及解决方案

Table 2　Advantages, limitations, and solutions of traditional LPBF and LDED techniques in heterogeneous metal manufacturing

Technique	Advantage	Limitation	Solution
LPBF	1) High forming accuracy 2) Higher quality of interface bonding	1) Lower processing efficiency[50] 2) Difficult to control the precise distribution of powder[51] 3) Cross-contamination issue with powders[52] 4) Intra-layer heterogeneous material composition connectivity is limited[53]	1) Hybrid manufacturing 2) Development of new powder spreading device 3) Developing multi-beam and large-area equipment 4) Upgrade of powder recycling unit
LDED	1) High degree of processing freedom 2) Wide selection of raw materials 3) High processing efficiency 4) Good flexibility in powder feeding	1) Lower forming accuracy[54] 2) Intra-layer heterogeneous material composition connectivity is limited[55]	1) Integration of additive and subtractive manufacturing processes 2) Hybrid manufacturing 3) Improvement of powder feeding and mixing device

3.1 基于激光定向能量沉积送粉系统

对于LDED工艺，基于其同轴送粉的原理，通过不同喷嘴进行原料（同种、异种或混合原料）的输送[56]，即可实现异质金属的直接或梯度连接［图4（a）］，因此只需增加料斗数量即可适配异质金属的增材制造。例如，Ostolaza等[57]通过双料斗LDED系统［图4（b）］，成功制备了AISI 316L/AISI H13异质金属梯度材料。韩国InssTek公司[44]研制的MX-Lab三轴多材料激光增材设备最多可容纳六个进料装置，能实现多种异质金属构件的直接或梯度连接，兼具高的加工及成分调控自由度。此外，将增减材复合制造技术集成至多材料LDED系统中，是提高成型质量颇具前景的方向。例如，DMG MORI[58]开发了一款LASERTEC 6600设备［图4（c）］，该设备将五轴铣削与激光沉积相结合，可实时监测工艺动态，能够在单个系统中为异质金属部件提供准确的形状控制，显著减少材料浪费并提高生产效率，适用于生产换热器、火箭喷管、涡轮机壳体等异质金属空天组件。LDED设备的改进还集中在混粉过程的优化上，以提高异质梯度构件的成型质量。例如，Chen等[59]在LMD设备中集成了一种静态混合器［图4（d）］，以实现异质粉末的快速、均匀混合，并通过流体力学计算、粒子混合仿真模型，以及316L/Cu的粉末混合实验，验证了这一方案的可行性。综上所述，目前LDED异质增材设备的改进方向主要集中在送粉方式、加工精度和原料状态等方面的优化。

3.2 基于激光粉末床熔化铺粉系统

对于LPBF来讲，由于传统的设备仅允许一次使用单一材料和有限的层间材料过渡，因此难以实现异质金属的连接，需要对送粉方式进行改进。例如，Daram等[60]通过增加传统刮刀式LPBF进料器的数量［图5（a）］，成功实现了Ni/Ti双金属梯度材料的制备，但这种方法无法实现*XY*向的层内异质材料连接。为了解决这个问题，Errico等[61]在原LPBF设备中开发了一个分区系统［图5（b）］，并将其放置在粉末室内，制备出了良好冶金结合的AISI 316L/镍基高温合金异质金属构件，证实了这一策略的可行性。Al-Jamal等[62]在SLM系统中集成了一个压电转换器振动进料系统［图5（c）］，通过超声振动的送料方式成功制造出二维H13/Cu多金属组件。但这种方法的缺点在于逐点送粉效率低，不适合大面积粉末铺设，且制造速度较慢。曼彻斯特大学[63]则集成了上述两类方法的优势，开发了一款刮刀结合超声辅助装备［图5（e）］，可以精确移除多余粉末，提高沉积效率并确保材料的精确沉积，成

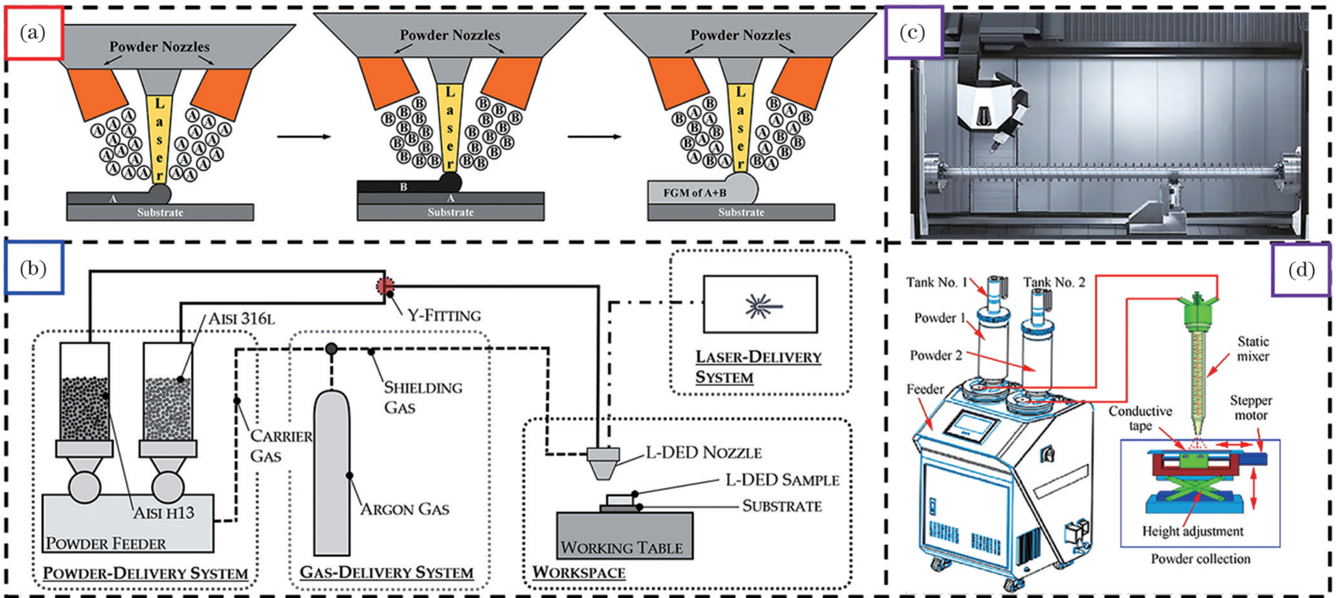

图4　LDED异质金属增材装备。(a)异质金属LDED增材制造工作原理示意图[56]；(b)双料斗LDED系统[57]；(c)LASERTEC 6600增减材复合装备[58]；(d)LMD静态混粉器设备示意图[59]

Fig. 4　LDED equipment for heterogeneous metal additive manufacturing. (a) Schematic of the working principle of LDED for heterogeneous metal additive manufacturing[56]; (b) dual hopper LDED system[57]; (c) LASERTEC 6600 additive-subtractive composite manufacturing equipment[58]; (d) schematic of LMD static powder mixer equipment[59]

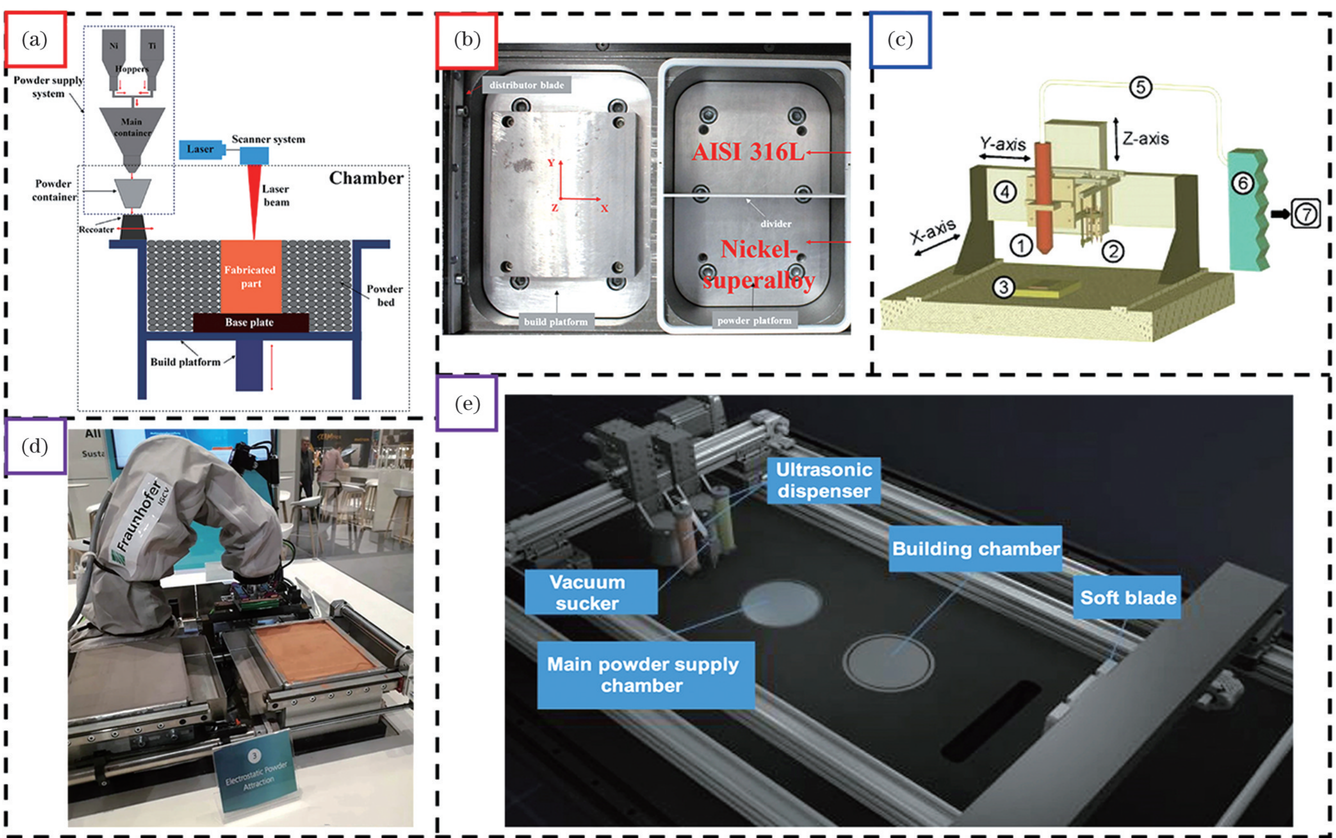

图5　LPBF异质金属增材装备。(a)双进料器LPBF装备[60]；(b)LPBF装备分区系统[61]；(c)超声波式LPBF送粉装置[62]；(d)静电式LPBF送粉装置[44]；(e)超声结合刮刀式LPBF装备[63]

Fig. 5　LPBF equipment for heterogeneous metal additive manufacturing. (a) Dual feeder LPBF equipment[60]; (b) zoning system for LPBF equipment[61]; (c) ultrasonic powder spreading device for LPBF[62]; (d) electrostatic powder spreading device for LPBF[44]; (e) blade-ultrasonic powder spreading equipment for LPBF[63]

功制备出316L/Cu10Sn二维双金属组件。此外，Fraunhofer IGCV研究所[44]研制了一款基于静电原理的送粉装置[图5(d)]，它可以适配各类铺粉式增材打印设备，可以快速、精确地形成所需的材料图案，并兼具层内异质材料连接的能力。SLM Solutions[44]、Aerosint[64]等公司近年来也开发出了基于铺粉-吸粉(SLM280 2.0)、转鼓式铺粉(AconityMIDI+)等新型LPBF装备，可在异质金属增材制造过程中实现高效粉末回收。表3汇总了目前LPBF及LDED的装备发展情况及相应的改进效果。

表3 LPBF及LDED异质金属增材装备发展及优势

Table 3 Development and advantages of heterogeneous metal additive manufacturing equipment for LPBF and LDED

Equipment Optimization Strategy	Technique	Material	Advantage/effect	Reference
Blade-based dual powder recoater	LPBF	Ni/Ti	Cracks and brittle phases exist at the interfacial joints; such technique is difficult to realize the deposition of heterogeneous materials in the same layer and are limited in the applicable material systems, with poor forming quality	[60]
Ultrasonic assisted powder spreading	LPBF	W/316L	Heterogeneous metals are well bonded; such technique has high powder layup accuracy and design freedom, but is very inefficient	[65]
Electrostatic powder spreading	LPBF		Such technique has a high degree of design freedom and powder feeding efficiency, but is prone to powder layer contamination problems	[63]
Blade + ultrasonic hybrid powder spreading	LPBF	316L/Cu10Sn	Good metallurgical bonding of heterogeneous metals; such technique combines high precision and efficiency	[66]
Dual powder feeder	LDED	AISI 316L/AISI H13	Individual transportation of dissimilar powders and successful bonding of heterogeneous metals are realized	[57]
Static mixing device	LDED	316L/Cu	Improved powder mixing homogeneity for the preparation of functional gradient layers	[59]
Integration of additive and subtractive manufacturing	LDED		Improved efficiency and precision of heterogeneous metal forming	[58]
Equipment improvement	LPBF	AISI 316L/Ni-based high-temperature alloy	Preparation of intra-layer bimetallic samples realized	[61]
	LPBF	AISI 316L-18Ni (300)	Preparation of intra-layer bimetallic samples realized	[67]

3.3 复合增材制造技术

在异质金属材料高效连接的方法中，多种增材工艺整合具有独特优势。例如，LDED兼具高的自由度和灵活性，电弧送丝增材制造(WAAM)技术可高效、低成本生产大尺寸构件，而LPBF则具有高的成型精度。然而，单一工艺在制备异质金属构件时也存在一些局限性，如LDED生产的样件表面质量较差，WAAM生产的样件易出现残余应力和变形问题，而LPBF由于装备限制在成型自由度上较差。通过多种工艺的耦合，不仅能够优化这些问题，提高双金属零件的生产质量和效率，还拓展了制造复杂几何形状和高性能构件的可能性。

Yoo等[68]通过LMD-WAAM工艺成功制备了IN625/SUS304L双金属梯度构件[图6(a)、(b)]，与单一方法相比，由LMD-WAAM所制备的样件具有高的沉积量以及低的缺陷密度。此外，在界面处异质金属结合良好，组织分布均匀，具有较高的抗拉强度。Ozsoy等[69]通过LPBF-WAAM工艺成功连接了17-4 PH与AISI 316L不锈钢[图6(c)]，构件界面处实现了可靠键合。通过后处理，构件可以获得良好的组织分布和力学性能。Zhang等[70]采用LPBF-LDED耦合工艺制备了中间层In718连接的QCr0.8铜合金/S06不锈钢异质金属构件[图6(d)]，在不同异质连接界面处实现了99.9%的高相对密度，实现了良好的冶金结合。这一复合制造的异质构件同样表现出均匀的组织分布及良好的力学性能。此外，德国Trumpf公司[44]先通过LPBF制备出具有复杂冷却通道的纯铜部件，然后利用LDED技术在铜部件表面镀上镍基高温合金，

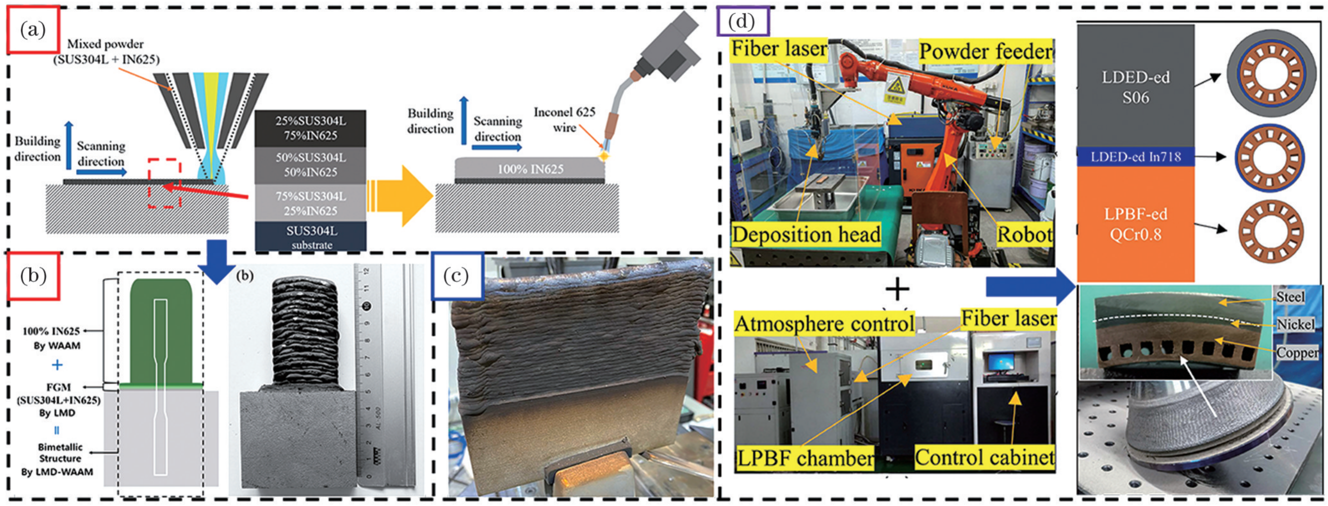

图 6 复合增材制造案例。(a)(b)LMD-WAAM 复合制造 IN625/SUS304L 梯度材料示意图及成型构件的宏观照片[68];(c)LPBF-WAAM 成型 17-4 PH/AISI 316L 样件示意图[69];(d)LPBF-LDED 装备,以及通过中间层 In718 实现 QCr0.8 铜合金/S06 不锈钢异质金属连接[70]

Fig. 6 Hybrid manufacturing cases. (a)(b)Schematic diagram of LMD-WAAM hybrid fabrication of IN625/SUS304L gradient material and macroscopic photographs of formed component[68]; (c) 17-4 PH/AISI 316L component formed by LPBF-WAAM[69]; (d) LPBF-LDED equipment, and QCr0.8 copper alloy/S06 stainless steel heterometal connection through the intermediate layer In718[70]

使成型构件兼具耐热及高强性质。Rodrigues 等[71]则采用 WAAM-LDED 工艺制备了 ER70S6/Inconel 625 双金属结构,界面处接合良好,未出现分层、孔隙、脆性有害相等组织缺陷,成型构件具有高的力学性能。表 4 汇总了目前复合制造技术应用于异质金属连接的相关研究及优势。

表 4 异质金属的复合制造技术及其优势

Table 4 Hybrid manufacturing processes for heterogeneous metals and their advantages

Technology integration strategy	Material	Advantage/effect	Reference
LMD-WAAM	SUS304L/IN625	Combines the high efficiency of WAAM with the flexibility of LMD/Good metallurgical bonding of heterogeneous materials with high mechanical properties	[68]
LPBF-WAAM	17-4 PH/ AISI 316L	Hybrid manufacturing facilitates the preparation of complex and large cross-section structures/Heterogeneous interfaces are well bonded and have high mechanical properties	[69]
LPBF-LDED	QCr0. 8/In718/ S06 stainless steel	Combines the high precision of LPBF with the flexibility of LDED/Heterogeneous interfaces are well bonded and defect-free	[70]
WAAM-LDED	ER70S6/Inconel 625	Combines the high efficiency of WAAM with the flexibility of LDED/Heterogeneous interfaces are well bonded and have high mechanical properties	[71]
LPBF-LDED	SS316L/IN625	Integration of LPBF for high forming accuracy and LDED for fast deposition/Good heterogeneous interface bonding	[72]
SLM-CS (cold spraying)	Al/Ti6Al4V	CS avoids defects associated with the melting process, SLM offers high forming accuracy/Better bonding at heterogeneous interfaces, and inhibits the generation of brittle phases	[73]

4 制造工艺及优化

界面决定了异质金属增材构件的性能及服役过程中的可靠性,因此获得良好冶金结合的异质界面是激光增材制造过程的关键。界面质量主要由材料相容性和工艺参数所共同决定,如图 7 所示。异质金属间复杂的物化性质差异(热膨胀系数、熔点、密度、表面张力、弹性模量和晶体结构不匹配等)和异质金属对激光

处理的响应差异会导致一系列的宏观及微观缺陷，例如孔隙、裂纹、有害相（脆性金属间化合物、氧化夹杂物）、残余应力等，需要从材料设计、连接方式、制造过程控制、前后端处理等多个方面进行综合考虑，以最大限度地提升异质界面的接合质量。图7介绍了激光增材制造过程中的各类缺陷及可能的解决方案。

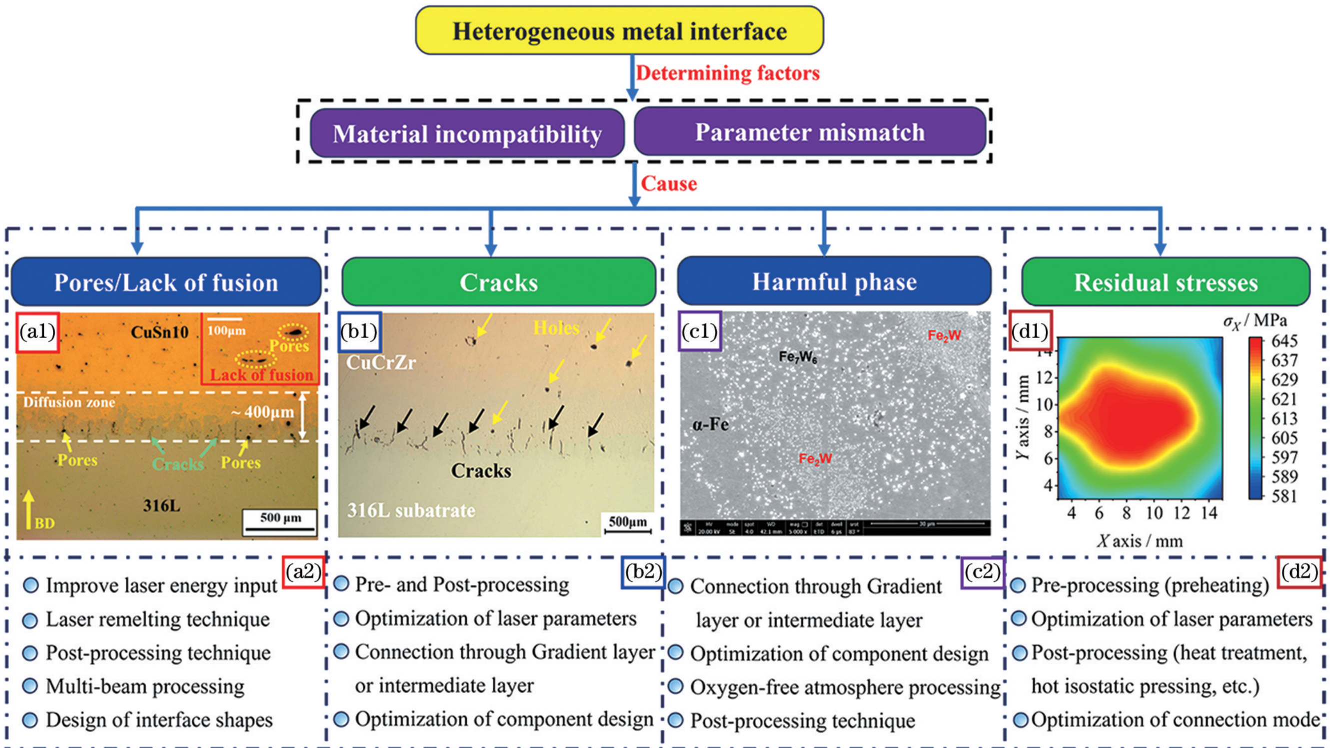

图7 异质金属界面质量的影响因素及优化方案。(a1)(a2)孔隙/粉末熔合不足[74]及解决方案；(b1)(b2)裂纹[75]及解决方案；(c1)(c2)有害相[38]及解决方案；(d1)(d2)残余应力[76]及解决方案

Fig. 7 Factors affecting the quality of heterogeneous metal interfaces and solutions. (a1)(a2) Porosity/lack of fusion[74] and related solutions; (b1)(b2) cracks[75] and related solutions; (c1)(c2) harmful phases[38] and related solutions; (d1)(d2) residual stresses[76] and related solutions

4.1 连接策略及参数调控

异质金属间固有的不相容性会导致各种界面问题，削弱结合部位的完整性和构件整体性能。为了实现多样化材料特性差异之间的可靠键合，近年来发展出了直接连接、过渡层、中间层和组合层4类连接方式[图8(a)][77]。

直接连接策略适宜于物化特性相似的金属，该方法复杂性和成本较低，利于制造同质性较高的双金属构件。但这种方法往往由于界面处突变较大，很容易引起界面失效。Wei等[19]采用直接连接策略制备了Cu10Sn/Ti6Al4V双金属结构，从成型样件中可以观察到明显的界面分层现象[图8(b)]，这证实直接连接并不适用于物化性质差异较大的异质金属。过渡层连接则通过建立金属之间的成分梯度，优化了结构的渐进性，可以有效解决界面不匹配的问题。这类策略可以实现界面处的均匀应力分布和可靠键合，尤其适用于需要缓解热和机械性能相差悬殊的材料组合，以防止界面缺陷的产生。Zhang等[78]通过LENS技术，成功制备了马氏体不锈钢/奥氏体不锈钢功能梯度材料[图8(g)]。相较于单组分马氏体不锈钢，连接后的双金属样件具有更优异的极限抗拉强度和伸长率。

通过配置中间层也是一类可靠的连接策略，可以阻止潜在脆性相的形成和裂纹扩展，显著提高物性差异较大金属间的结合能力。为了消除有害Fe-Ti金属间化合物的形成，Tey等[79]在Ti6Al4V与SS316不锈钢之间添加了Cu10Sn合金中间层，有效改善了异质接合界面的质量，并通过微观组织的调控，获得了高强度、高韧性和高稳定性的多金属构件[图8(e)]。组合层策略是指将目标材料与第三种兼容材料混合，进而实现异质材料间的高效连接。由于Inconel 718与Ti64在热性能上的不匹配，以及它们在界面上容易形成脆性金属间相，这两者的组合可能导致结构分层。为了成功制造异质金属构件，Onuike等[80]使用了一种混合第三种材料（VC）的成分组合键合层（CBL）。该组合键合层作为中间层连接两种不互溶的合金，从而获得了无裂纹、无脆性金属间化合物、低界面热应力的双金属结构[图8(f)]。

界面设计同样是优化异质金属连接的重要策略。图8(c)为Wei等[81]通过SLM制备的"指状交叉"

316L/CuSn10异质金属界面结构。这类特殊的界面设计有利于增强元素扩散，并提高了界面接合质量和结合强度。Li等[82]通过LDED技术设计和制备了一种双金属SS316L/IN625仿生异质结构材料(BHM)。这种结构可以减少两种材料之间的界面不匹配，有利于应力传递和载荷分布，提高材料的机械性能，并兼具优异的塑韧性[图8(d)]。表5汇总了异质金属的连接策略、案例及相应的成型效果。

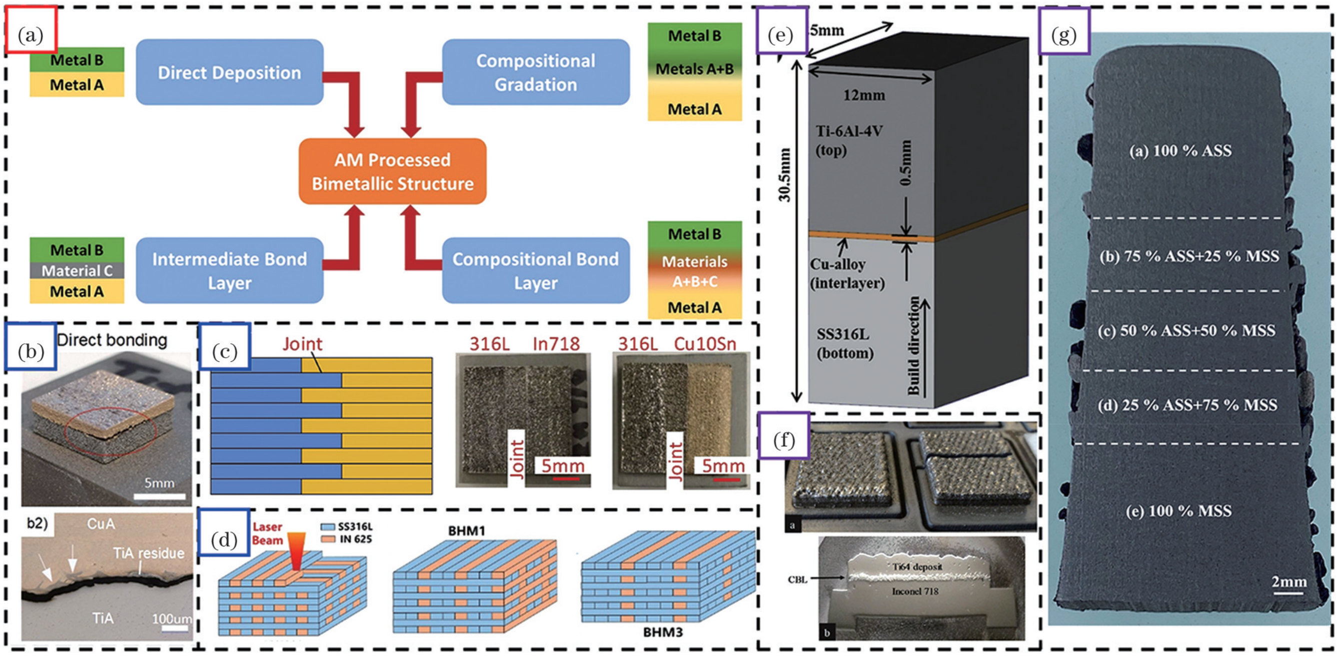

图8 异质金属连接策略及案例。(a)四类连接策略示意图[77]；(b)LPBF直接连接Cu10Sn/Ti6Al4V及其界面情况[19]；(c)SLM成型的指状交叉316L/CuSn10界面结构及成型样品[81]；(d)LDED成型的仿生SS316L/IN625界面结构[82]；(e)SLM通过中间层Cu10Sn合金实现Ti6Al4V/SS316异质金属的连接[79]；(f)LENS通过VC-Inconel 718-Ti64组合键合层实现Inconel 718/Ti64的连接[80]；(g)LENS通过梯度过渡层连接马氏体不锈钢/奥氏体不锈钢[78]

Fig. 8 Heterogeneous metal joining strategies and cases. (a) Schematic diagrams of the four types of joining strategies[77]; (b) LPBF direct joining of Cu10Sn/Ti6Al4V and its interface[19]; (c) finger-crossed 316L/CuSn10 interfacial structure and samples formed by SLM[81]; (d) bionic SS316L/IN625 interface structure formed by LDED[82]; (e) Ti6Al4V/SS316 stainless steel heterometal connection through the intermediate layer Cu10Sn using SLM[79]; (f) inconel 718/Ti64 heterometal connection through VC-Inconel 718-Ti64 combination bonding layer using LENS[80]; (g) martensitic stainless steel/austenitic stainless steel connection through gradient layer using LENS[78]

在异质金属连接中，考虑到不同金属的熔点、导热系数和热膨胀系数等物化性质存在差异，仅仅以单一材料的适配参数可能无法满足异质金属连接质量和最终性能要求。因此，有必要深入研究并调控合适的激光参数，以优化组织、消除缺陷，并提升异质金属构件的整体质量。在LPBF过程中，一般用体积能量密度(D_{VED})来量化输入粉层的激光能量[28]：

$$D_{\mathrm{VED}}=\frac{P}{v\times h\times z},\tag{1}$$

式中：P代表激光功率；v为扫描速度；h为扫描间距；z代表粉层厚度。此外，LDED过程中的激光能量输入也可用能量密度(D_{ED})进行量化[76]：

$$D_{\mathrm{ED}}=\frac{P}{k\times Q\times v\times d\times(1-\omega)},\tag{2}$$

式中：Q代表送粉速率；k为量纲常数；ω代表重叠率；d为激光束直径。Liu等[76]通过LMD工艺制备了GH4169/K417G梯度双金属结构，通过正交实验首先确定了GH4169基底的最优工艺参数(扫描速度、送粉速率和重叠率)。在此基础上，通过调节激光功率进而研究体积能量密度对于双金属梯度构件孔隙率的影响[图9(a)]。从图中可以看到，适中的能量输入可以保证构件高水平的相对密度值。此外，为了解决传统LMD制造过程中异质材料的参数匹配问题，Wang等[90]提出了一种综合考虑粉体分离、缺陷和功耗的工艺参数筛选策略[图9(b)]，并将原本需要的参数调优实验量缩减至一半左右。通过这种方法，该团队成功得到最优工艺参数，并制备出无缺陷、高抗拉强度的IN625/304L双金属功能梯度构件。Wu等[30]通过LPBF工艺制备了Ti6Al4V/AlSi10Mg双金属结构，并发现高能量密度(对应于高激光功率和低扫描速度)输入会导致界面裂纹和成型失效[图9(c)]，而低能量输入则会导致孔隙缺陷，这主要是因为激光对于粉末熔化不完全，合适的

表 5 异质金属的连接策略及成型效果

Table 5 Joining strategies and forming effects of heterogeneous metals

Connection strategy	Material	Technique	Effect	Reference
Direct connection	Cu10Sn/Ti6Al4V	LPBF	Interface delamination, bonding failure	[19]
	Cu/SS 304L	LDED	High residual stresses at the interface, poor bonding effect	[83]
Gradient layer connection	Martensitic stainless steel/Austenitic stainless steel	LENS	Good metallurgical bonding, improved mechanical properties	[78]
	316L/IN718	LPBF	Good metallurgical bonding, good mechanical properties	[84]
	AISI 316L/Fe35Mn	LPBF	Good metallurgical bonding, mechanical properties vary with composition gradation	[85]
	316L/Inconel 625	LDED	Good metallurgical bonding, uniform microstructure at the interface	[22]
	Ti6Al4V/NiTi	LDED	Defect-free interface structure and good mechanical properties	[86]
Intermediate layer connection	316L/HOVADUR K220/Ti-6Al-4V	SLM	Good metallurgical bonding	[79]
	Cu10Sn/316L/W	LPBF	Good metallurgical bonding	[37]
	TC4/Cu/IN718	LDED	Inhibits the creation of defects, good interfacial bonding	[87]
	IN625/Cu/TC4	LDED	Good metallurgical bonding	[88]
	Ti6Al4V/Cu/Al-Cu-Mg	LPBF	Good metallurgical bonding, no visible defects	[89]
Compositional bond layer connection	Inconel 718/VC mixture/Ti6Al4V	LENS	No cracks in the interface, successful bonding	[80]
Interface shape design	316L/CuSn10	SLM	Good metallurgical bonding, improved mechanical properties	[81]
	316L/IN625	LDED	Good bonding, improved mechanical properties	[82]

能量输入则可以保证异质金属间的良好冶金结合。Song 等[12]利用 SLM 进行了 NiTi/CuSn10 的增材连接，在高扫描速率（300、350 mm/s）下，沿着扫描路径方向会产生大的温度梯度和热应力，进而会诱发从 NiTi 基底扩展的垂直微裂纹。当扫描速度和激光功率适中时，界面质量优，未发现明显缺陷。而随着能量密度的提高，熔池的运动变得逐渐强烈，并生成了岛状区域、大孔隙和裂纹等缺陷[图 9（d）]。从上述案例可以发现，过低或过高的激光能量输入均会导致不同程度的缺陷，因此基于异质金属的特性，通过合理调控参数组合，进而获得适合的激光能量输入，是实现异质金属良好键合的关键。表 6 汇总了一些经典异质材料体系的最优/适配激光工艺参数。

4.2 在线监测及智能预测

在增材制造过程中，异质金属结构的制备因涉及多种材料和复杂的热效应而展现出极大的复杂性和不确定性。通过实时监测技术和模拟预测工具来实现制造过程的高效控制，是获得可靠异质界面的重要手段。

目前异质金属激光增材在原位监测领域的研究较少，主要集中于反应过程的监测。Prasad 等[99]通过在 LMD 设备上集成高速成像装置[图 10（a）]，观察了铜、铝、钢在钛合金上的沉积过程，分析了熔池演变过程，并比较了各金属沉积过程中熔池的行为差异[图 10（b）]。Wasmer 等[100]设计了一种新型在线监测系统[图 10（c）]，通过使用光发射光谱传感器以及七种主流人工智能算法，成功实现了对梯度材料化学成分和工艺状态的高精度监测。此

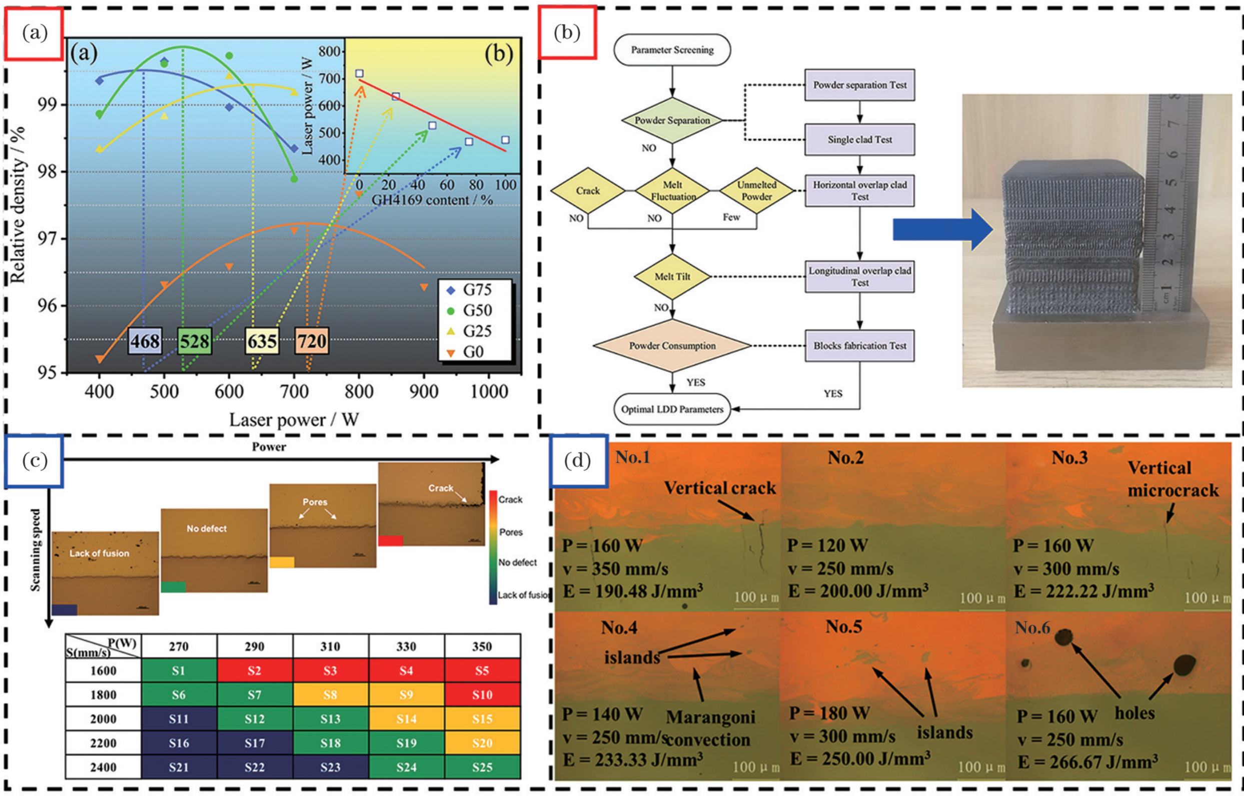

图9　工艺参数对异质金属构件的组织性能影响。(a)LMD成型的GH4169/K417G异质金属构件相对密度随激光功率的变化[76]；(b)LMD的工艺参数优化策略及最优参数下制备的IN625/304L异质金属构件[90]；(c)在不同工艺参数下，LPBF成型的Ti6Al4V/AlSi10Mg异质界面情况[30]；(d)在不同工艺参数下，SLM成型的NiTi/CuSn10异质界面情况[12]

Fig. 9　Influence of process parameters on the microstructure and properties of heterogeneous metal components. (a) Variation of the relative density of LMD-formed GH4169/K417G heterogeneous metal components with laser power[76]; (b) LMD parameter optimization strategy and IN625/304L heterogeneous metal components prepared under the optimal parameters[90]; (c) Ti6Al4V/AlSi10Mg heterogeneous metal interfaces formed by LPBF under different process parameters[30]; (d) NiTi/CuSn10 heterogeneous metal interfaces formed by SLM under different process parameters[12]

表6　经典异质材料体系的最优/适配工艺参数

Table 6　Optimization/processing parameters for classical heterogeneous material

Material	Technique	Laser power /W	Scanning speed /(mm/s)	Scanning space /overlap rate	Layer thickness /μm	Powder feeding rate	Reference
Ti6Al4V/ AlSi10Mg	LPBF	310	2200	0.12	30		[30]
Ti6Al4V/Inconel 625	LMD	1500	600	50%		6.0 g/min	[91]
Ti6Al4V/Ti48Al2Cr2Nb	LMD	1900	7			4.96 g/min	[92]
Ti6Al4V/NiTi	SLM	90	600	0.09	30		[26]
Ti6Al4V/IN718	SLM	300	700	0.05	50		[93]
316L/Co-Cr-Mo	LENS	800	6.67			6.0 g/min	[36]
316L/IN718	LPBF	95	500	0.084	25		[84]
316L/Hastelloy X	LPBF	95	200	0.045	30		[94]
316L/IN718	LDED	1000	7	50%		1 r/min	[95]
316L/TC4	LMD	1400	6	50%		2.5 r/min	[96]
Inconel 718/316L	LPBF	300	900	0.08	30		[97]
Inconel 718/CoCrMo	LPBF	225	700				[34]
Inconel 718/SS420	LDED	900	15				[23]
Inconel 625/316L	LENS	335	18			3.8 g/min	[98]
Inconel 625/304L	LMD	600	10	50%		8 g/min	[90]
GH4169/K417G	LMD	528	4	40%		18.9 mm^3/s	[76]
NiTi/CuSn10	SLM	120	250	0.08	30		[12]

外，他们指出声发射不适用于LDED过程中激光-材料相互作用的监测，因为声信号在传播过程中会受到高度屏蔽和干扰。Chen等[101]利用高速X射线成像技术对LPBF成型的Inconel 718/316L进行了原位观察[图10(d)、(e)]，可实现组织缺陷演变及熔池热行为的实时监控，这一策略可辅助异质金属增材过程中的工艺及参数调控。Chen等[102]将光学装置耦合至LDED设备中[图10(f)]，通过等离子体光谱信号，实时监控了316 L/AlSi10Mg双金属梯度构件在制造过程中的梯度成分演变，这一方案可用于增材过程中的成分调控。表7根据检测信号的类型，对于目前异质金属激光增材过程中的原位监测技术进行了梳理，并指出了各类方案的优势和效果。

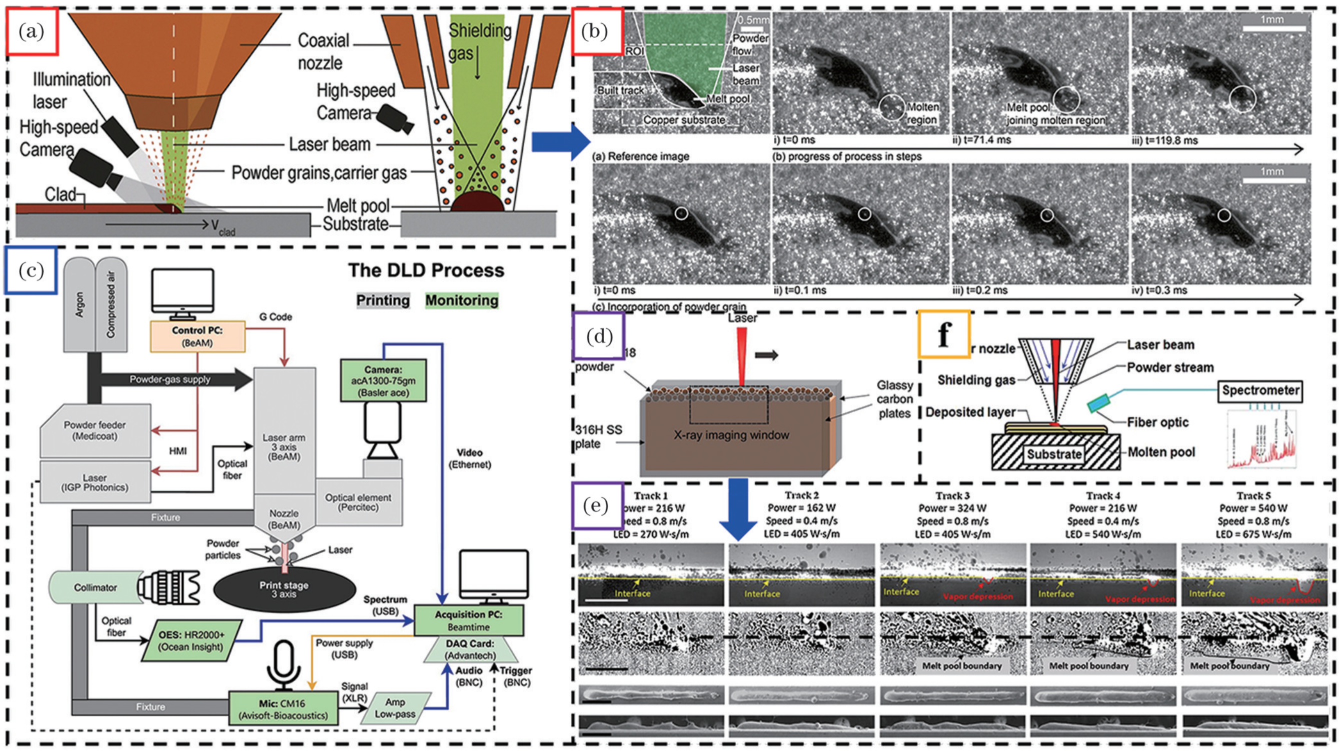

图10 异质金属激光增材在线监测技术的发展和应用。(a)(b)LMD设备集成高速成像装置示意图及Cu沉积过程的高速成像图片[99]；(c)集成监测传感装置后的LDED系统[100]；(d)(e)集成至LPBF系统中的原位X射线成像实验装置示意图及不同加工参数下所捕获Inconel 718/316L成型过程照片[101]；(f)LDED系统集成光学装置示意图[102]

Fig. 10 Development and application of online monitoring technology for LAM preparation of heterogeneous metals. (a)(b) Schematic diagram of the integrated high-speed imaging device of the LMD equipment and high-speed imaging pictures of the Cu deposition process[99]; (c) LDED system with integrated monitoring and sensing device[100]; (d)(e) schematic diagram of the in-situ X-ray imaging device integrated into the LPBF system and the photos of the Inconel 718/316L forming process captured under different processing parameters[101]; (f) schematic diagram of integrated optical device for LDED systems[102]

数值模拟、机器学习等智能预测方法在异质金属激光增材中有助于增进复杂过程的理解。通过这些方法，可以优化工艺参数，预测产品性能，尤其是在处理异质金属结构时，能够显著提高制造效率和成品质量，减少试错成本。Kumar等[103]开发了一个顺序耦合热机械模型[图11(a)]，揭示了激光增材制造过程中多组分IN718/Ti6Al4V系统的热响应、凝固行为及残余应力形成机制，并结合实验验证了该模型的可靠性。Miao等[104]通过机器学习方法优化了AlSi10Mg/316L异质金属的SLM工艺参数[图11(b)]，并使用高斯过程回归模型成功预测不同激光功率和扫描速度对部件密度和表面粗糙度的影响，为异质金属增材制造的参数优化提供了一个新的方案。Sun等[105]通过开发一种介观尺度的多相模型，揭示了LPBF制造IN718/Cu10Sn异质结构时的熔池行为和凝固轨迹形态[图11(c)]，并提出了如何适应性调整搭接间距以确保熔融带之间充分熔合，从而提高异质金属间的打印质量。Li等[83]通过实验结合热力学有限元分析模型，研究了LDED工艺中直接沉积和分阶段沉积Cu/SS304L梯度结构的残余应力和变形现象[图11(d)]，验证了通过引入梯度层可以成功实现无缺陷的异质金属接合，为优化异质金属梯度构件的设计和材料选择提供了一种高效的预测方法。表8基于预测内容的类型，对目前异质金属激光增材过程中的仿真模拟、机器学习相关研究进行了总结，并指出了各类方案的优势和效果。

表7 异质金属激光增材制造的监测技术

Table 7 Monitoring techniques for laser additive manufacturing of heterogeneous metals

Monitor signal	Material	Technique	Monitoring device	Advantage/effect	Reference
Optical signal	Cu, Al, Steel/Ti alloy	LMD	High-speed camera (optical imaging)	Real-time monitoring of the melt pool dynamics, powder status and solidification characteristics, which can be adjusted accordingly	[99]
	Ti/Nb	LDED	Spectrum collection device	High precision monitoring of chemical composition/process status/serious defects	[100]
	Inconel 718/316L	LPBF	High-speed X-ray imaging device	It can realize real-time monitoring of microstructure and defect evolution as well as thermal behavior of molten pool, and can adjust the process accordingly	[101]
	316 L/AlSi10Mg	LMD	Collimating lens + optical fiber (spectral collection)	The relationship of spectral intensity-gradient composition evolution can be established to realize composition control in manufacturing process	[102]
Acoustic signal	Ti/Nb	LDED	Microphones	For laser-material interaction monitoring with high acquisition rates but poor monitoring accuracy	[100]

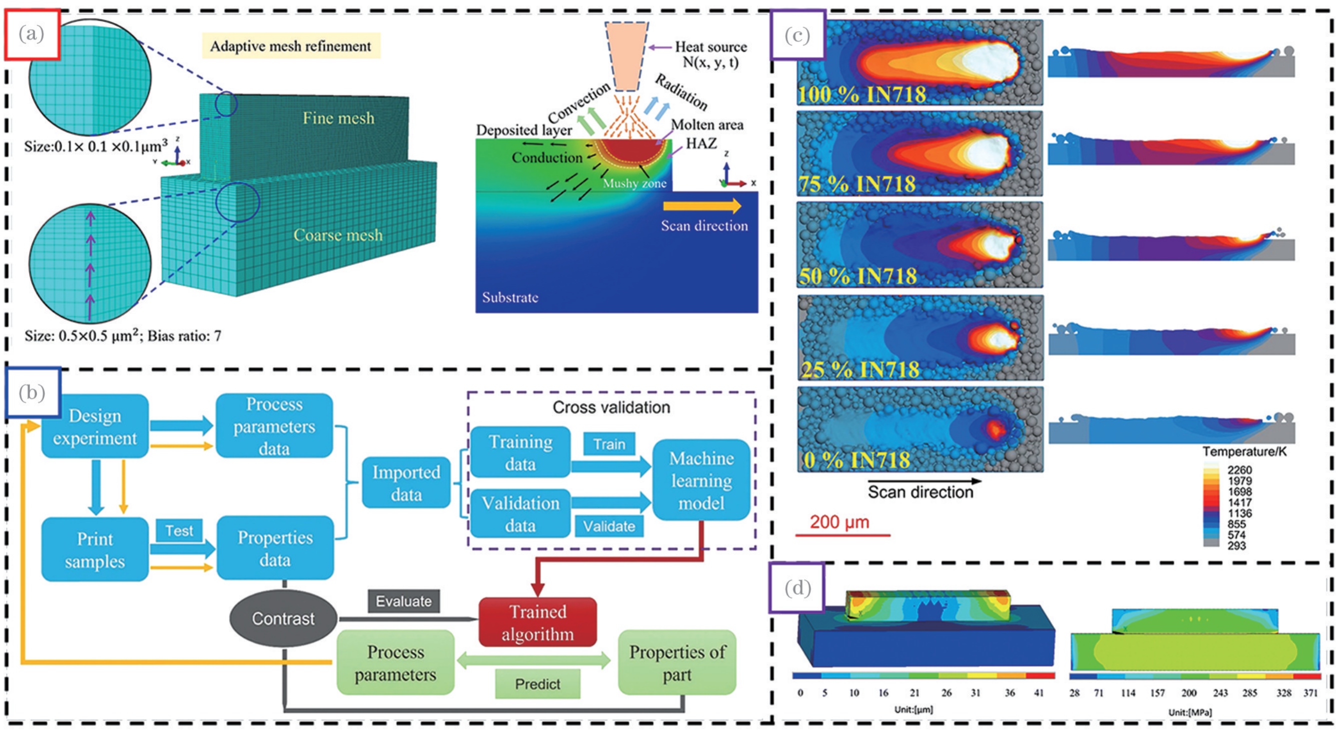

图11 异质金属激光增材模拟技术的发展和应用。(a)LDED建模自适应网格及用于热分析的边界条件[103];(b)SLM参数优化的机器学习流程图[104];(c)LPBF成型IN718/Ti6Al4V过程中不同梯度IN718组分的粉床温度分布模拟图[105];(d)LDED成型Cu/SS304L的变形及应力分布模拟[83]

Fig. 11 Development and application of simulation technique for LAM preparation of heterogeneous metals. (a) LDED modeling adaptive mesh and boundary conditions for thermal analysis[103]; (b) machine learning flowchart for SLM parameter optimization[104]; (c) simulation of powder bed temperature distribution with different gradient IN718 components during LPBF manufacturing of IN718/Ti6Al4V[105]; (d) simulation of deformation and stress distribution in LDED manufacturing of Cu/SS304L[83]

4.3 预处理及后处理

界面处不良的凝固动态和相变可能导致缺陷和各类有害相的形成,从而削弱材料的机械性能和服役可靠性。因此,除了精确控制过程参数和优化连接策略以外,材料预处理和后处理技术同样是优化材料组织性能的关键手段。

表8　异质金属激光增材的仿真模拟技术

Table 8　Simulation and modeling techniques for laser additive manufacturing of heterogeneous metals

Forecast content	Material	Technique	Model/method	Advantage/effect	Reference
Thermal behavior + residual stress	IN718/Ti6Al4V	LDED	Sequential coupled thermo-mechanical model	The predicted results are qualitatively in agreement with the experimental results / thermal response, solidification behavior and residual stress sources can be predicted	[103]
	Cu/SS304L	LDED	Thermo-mechanical Finite Element Modeling	Accurate prediction of temperature and residual stress distribution can be achieved	[83]
	IN718/Cu10Sn	LPBF	Mesoscopic modeling based on the VOF method	The behavior of molten pool and solidification trajectory can be predicted	[105]
	316L/Inconel 718	LDED	Finite element simulation	High simulation accuracy for effective analysis of thermal behavior during the forming process	[106]
	TC4/TC11	LMD	Finite element simulation	The temperature field trend, period and peak temperature calculated by the model are in good agreement with the experiment, which verifies the validity of the model	[107]
Process parameters	AlSi10Mg/316L	SLM	Gaussian process regression (MO-GPR) modeling	Process parameter optimization can be significantly shortened	[104]
	Fe/Ni	LDED	Mathematical models constructed based on MATLAB	Correlating laser process parameters to composition states	[108]
	316L/Cu	SLM	Multivariate Gaussian process model	Can be used for parameter prediction under different gradient composition changes	[109]

基材预热作为激光增材制造的一类关键预处理方法，其可通过调控温度来优化熔池动态和后续冷却路径。通过适度预热，可以降低增材制造过程中的热应力，减缓熔池冷却速度，从而有助于微观结构的均匀化，并减少裂纹形成的风险。Wei 等[110]利用 LDED 技术，以 10% 的成分间隔制备了 Inconel 625/Ti6Al4V 功能梯度双金属构件。通过在不同沉积阶段进行预热处理[图 12(a)]，制备的样件在成型效果上要明显优于未预热的样品[图 12(b)、(c)]。这是因为预热改变了组织的演化过程，避免了原本沉积过程中过渡区大量 Cr、Mo 富集相的生成，进而避免了裂纹的萌生。Pellizzari 等[111]通过 LMD 工艺制备了 CuBe/H13 双金属构件，发现基底预热可以实现组织和成分的调控，且抑制了孔隙与裂纹的产生[图 12(d)、(e)]，并对于表面硬度及耐磨性也有显著的提升效果。Liu 等[76]通过 LMD 工艺制备了 GH4169/K417G 梯度材料，通过测试发现样品顶面沿 X 轴的残余应力分布随基体预热温度的提高显著减小[图 12(f)、(g)]，这主要是由于熔池与周围环境之间的热梯度减小，改善了不均匀收缩的现象，进而使得残余应力减小。此外他们还发现随着预热温度的提升，材料在 YZ 平面的相对密度呈线性增长，这是由于预热提高了激光的吸收率，改善了润湿条件，并延长了熔融材料的凝固时间，进而提高了相对密度[图 12(h)]。

异质金属间存在热和机械不匹配，往往会导致残余应力、微观缺陷等问题，并残留至最终成型件中，严重影响其服役可靠性。因此需要通过后处理手段来进行优化和调控，提高构件的可靠性。Wen 等[112]通过 LPBF 制备了 316L/Inconel 718 双金属构件，并通过后续热处理调控组织分布，提高屈服强度和抗拉强度，但会降低其延展性[图 13(a)、(b)]。Pasco 等[113]的研究表明，适当的热处理可以稳定 LPBF 制备马氏体时效钢/Co-Cr-Mo 合金的多相界面，有助于改善合金的韧性、缓解残余应力并促进界面结构的均质化。此外可以促进合金界面的多相结构转变为均匀的平行马氏体结构，这有利于提高异质构件的强度和延展性[图 13(c)]。Borisov 等[114]通过 LPBF 制备了 Ti/Ti64 双金属梯度构件，通过后续热处理和热等静压处理发现硬度值有所下降[图 13(d)]，这主要是因为后处理过程促进了马氏体相分解以及应力消除，进而提升了材料的塑韧性。表 9 总结了异质金属激光增材的预处理和后处理方案以及对于构件的组织性能影响。

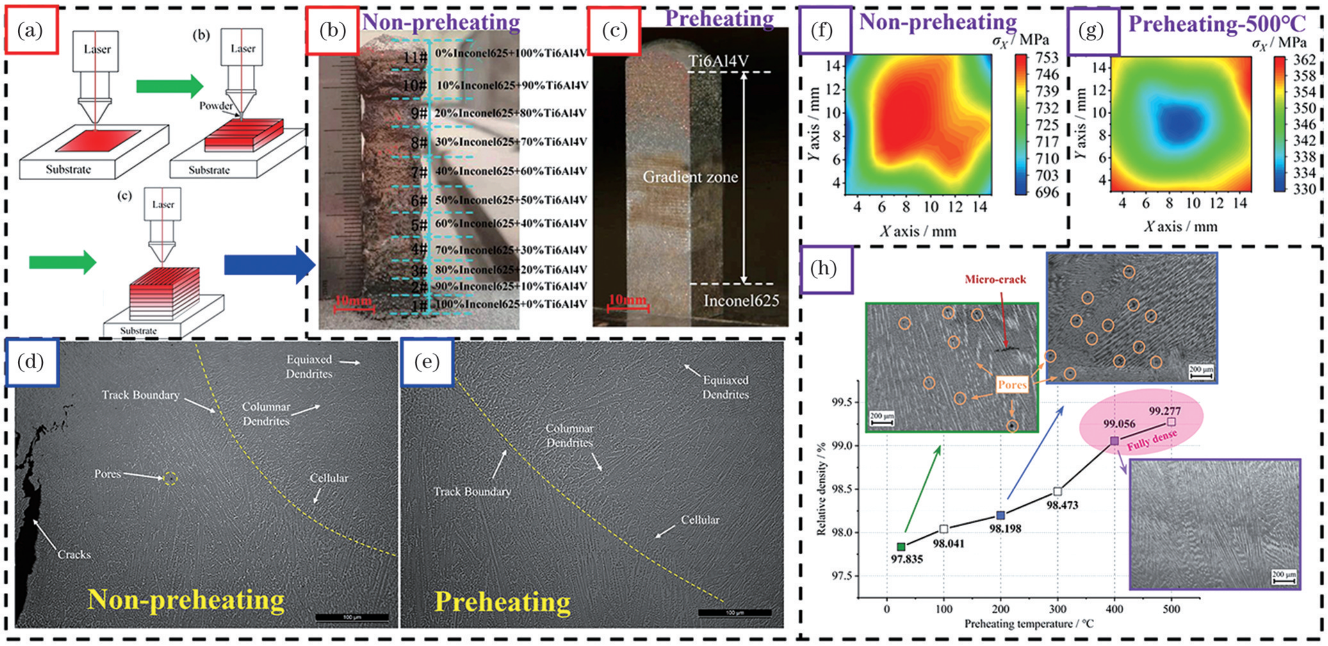

图 12 预处理对于异质金属构件组织性能的影响。(a)～(c)LDED 制造 Inconel 625/Ti6Al4V 梯度材料过程中的预热方法及有无预热成型样件效果对比[110]；(d)(e)有无预热条件下 LMD 成型 CuBe/H13 微观结构对比[111]；(f)～(h)有无预热条件下，LMD 成型 GH4169/K417G 样件的硬度、相对密度及组织变化[76]

Fig. 12 Effect of pretreatment on microstructure and properties of heterogeneous metal components. (a)–(c) Preheating process of LDED in the manufacture of Inconel 625/Ti6Al4V gradient materials and the comparison of the effect of forming samples with or without preheating[110]; (d)(e) comparison of microstructures of CuBe/H13 formed by LMD with or without preheating[111]; (f)–(h) hardness, relative density, and microstructure of GH4169/K417G samples formed by LMD with or without preheating[76]

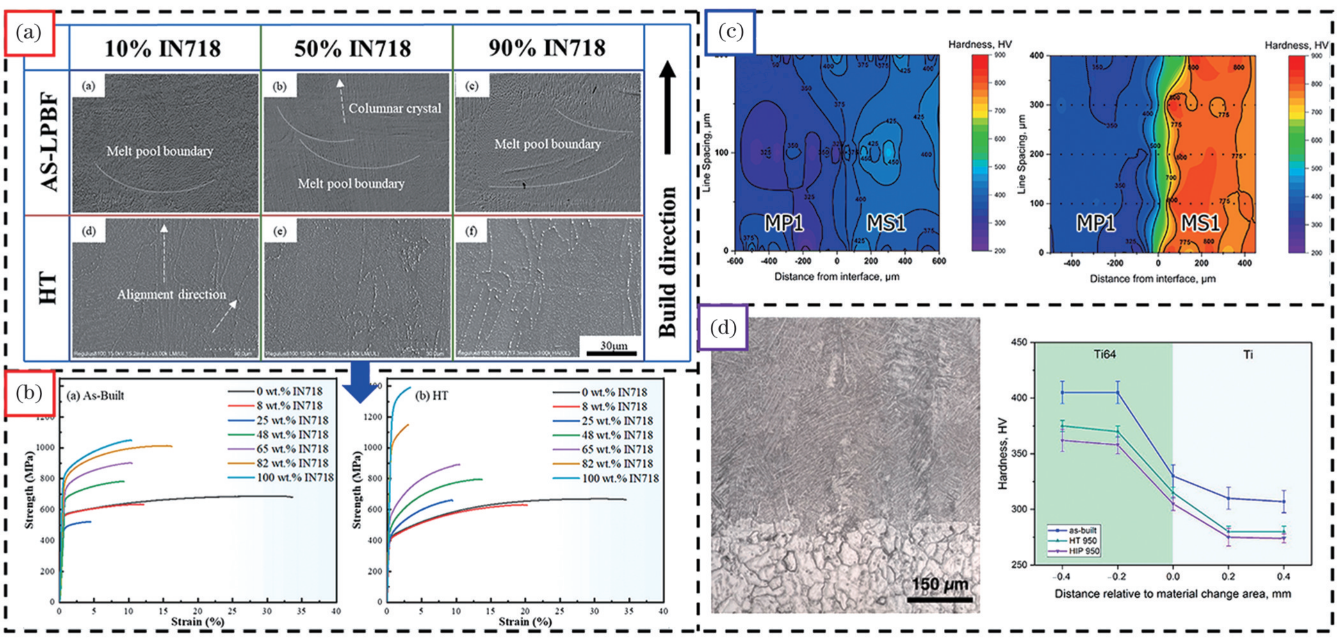

图 13 后处理对于异质金属构件组织性能的影响。(a)(b)热处理对于 LPBF 成型 316L/Inconel 718 构件的组织及机械性能影响[112]；(c)热处理对于 LPBF 成型马氏体时效钢/Co-Cr-Mo 合金构件的硬度影响[113]；(d)热等静压对于 LPBF 成型 Ti/Ti64 的组织及硬度影响[114]

Fig. 13 Effect of post-treatment on microstructure and properties of heterogeneous metal components. (a)(b) The effect of heat treatment on the microstructure and mechanical properties of LPBF-formed 316L/Inconel 718 components[112]; (c) the effect of heat treatment on the hardness of LPBF-formed maraging steel/Co-Cr-Mo alloy components[113]; (d) the effect of hot isostatic pressing on the microstructure and hardness of LPBF-formed Ti/Ti64 components[114]

表9 激光增材制造异质金属的预处理和后处理方案

Table 9 Pre- and post-treatments for laser additive manufacturing of heterogeneous metals

Processing method	Material	Technique	Effect	Reference
Substrate preheating	Inconel 625/Ti6Al4V	LDED	Optimized microstructure and improved forming quality	[110]
	CuBe/H13	LMD	Inhibit the formation of defects and improve mechanical properties	[111]
	GH4169/K417G	LMD	Reduced residual stresses and increased relative density of samples	[76]
Heat treatment	316L/Inconel 718	LPBF	Modulation of microstructure distribution to improve mechanical properties	[112]
	Maraging steel/Co-Cr-Mo	LPBF	Elimination of residual stresses, improvement of interface quality and toughness	[113]
	In718/316L	LDED	The strength and toughness of the components are improved	[115]
Hot isostatic pressure	Ti/Ti64	LPBF	Elimination of residual stresses and improvement of mechanical properties	[114]

5 展望与结束语

本文主要回顾了近年来异质金属激光增材技术的应用、装备，以及工艺研究的现状，并对其制约性问题及相关解决方案进行了探讨。异质金属激光增材技术正朝着多样化、集成化的方向发展，下面是对这一技术未来发展方向的展望和探讨：

1）激光增材制造设备的发展将聚焦于多金属材料的精准输送和调控，保障材料在成形过程中的均质性和稳定性。此外，还需要开发多光束-多材料激光打印系统，提高打印幅面尺度，开发兼具高精度和高灵活性的送粉技术，以适配大尺寸复杂构件的高效生产。多种工艺的整合（增减材复合、多种增材工艺复合）将带来更自动化和模块化的解决方案，以大幅提高生产效率和成型质量。

2）对于实现异质金属的高质量连接，精确的工艺参数调控至关重要。未来的发展将侧重于发展高级控制算法和自适应扫描策略，以考虑和协调金属材料间的热物理特性差异。例如，机器学习可以预测和优化粉末流动、能量输入和熔池稳定性，以减少缺陷和改进界面结合质量。此外，借助相图计算和模型预测等手段，通过优化异质金属的组分设计，开发新型连接策略（例如多组分组合键合层），设计新型界面接合形状，以最大限度地提高异质金属间的结合能力。

3）在线监测系统的发展将倾向于原位、非破坏性技术，例如高分辨率摄像监测、热像仪及X射线传感器等，这些技术能够实时跟踪异质结合界面及梯度区域的热分布和微观结构演化，并通过机器学习方法实现高效闭环控制。智能预测也会成为制造过程中的关键，利用大数据和先进的计算模型来精确预测材料的行为及制造参数，并确保成型件符合质量要求。为保障异质金属构件的整体性能和寿命，预处理和后处理步骤也将更加重要。将先进的改性技术应用于制造过程的前后端，例如激光喷丸、电化学抛光、激光冲击强化等，有利于获得更高质量的异质金属成型构件。

参 考 文 献

[1] Mehrpouya M, Tuma D, Vaneker T, et al. Multimaterial powder bed fusion techniques[J]. Rapid Prototyping Journal, 2022, 28(11): 1-19.

[2] Han P L. Additive design and manufacturing of jet engine parts[J]. Engineering, 2017, 3(5): 648-652.

[3] Piscopo G, Iuliano L. Current research and industrial application of laser powder directed energy deposition[J]. The International Journal of Advanced Manufacturing Technology, 2022, 119(11): 6893-6917.

[4] Guan J R, Wang Q P. Laser powder bed fusion of dissimilar metal materials: a review[J]. Materials, 2023, 16(7): 2757.

[5] Wang D, Liu L Q, Deng G W, et al. Recent progress on additive manufacturing of multi-material structures with laser powder bed fusion[J]. Virtual and Physical Prototyping, 2022, 17(2): 329-365.

[6] Tan C L, Chew Y, Bi G J, et al. Additive manufacturing of steel-copper functionally graded material with ultrahigh bonding strength [J]. Journal of Materials Science & Technology, 2021, 72: 217-222.

[7] 邓呈敏，程东海，张华，等. 铝/铜异种材料直流磁场辅助电弧熔钎焊研究[J]. 稀有金属，2021, 45(10): 1178-1184.
Deng C M, Cheng D H, Zhang H, et al. Study on aluminum-copper dissimilar materials by DC magnetic field assisted arc welding-brazing joint[J]. Chinese Journal of Rare Metals, 2021, 45 (10): 1178-1184.

[8] Hinojos A, Mireles J, Reichardt A, et al. Joining of Inconel 718 and 316 Stainless Steel using electron beam melting additive manufacturing technology[J]. Materials & Design, 2016, 94: 17-27.

[9] Sanjeeviprakash K, Kannan A R, Shanmugam N S. Additive manufacturing of metal-based functionally graded materials: overview, recent advancements and challenges[J]. Journal of the Brazilian Society of Mechanical Sciences and Engineering, 2023, 45(5): 241.

[10] Li S H, Kumar P, Chandra S, et al. Directed energy deposition of metals: processing, microstructures, and mechanical properties[J]. International Materials Reviews, 2023, 68(6): 605-647.

[11] Onuike B, Bandyopadhyay A. Bond strength measurement for additively manufactured inconel 718- GRCop84 copper alloy bimetallic joints[J]. Additive Manufacturing, 2019, 27: 576-585.

[12] Song C H, Hu Z H, Xiao Y M, et al. Study on interfacial bonding properties of NiTi/CuSn10 dissimilar materials by selective laser

melting[J]. Micromachines, 2022, 13(4): 494.

[13] Zhang B P, Xiao H F, Zhang W Q, et al. Influence of the thermal conductivity of different CuCr0.8 substrate state on the formability of laser directed energy deposition Inconel718 single track[J]. Materials Characterization, 2023, 202: 113015.

[14] Chen J, Yang Y Q, Song C H, et al. Interfacial microstructure and mechanical properties of 316L/CuSn10 multi-material bimetallic structure fabricated by selective laser melting[J]. Materials Science and Engineering: A, 2019, 752: 75-85.

[15] Bai Y C, Zhang J Y, Zhao C L, et al. Dual interfacial characterization and property in multi-material selective laser melting of 316L stainless steel and C52400 copper alloy[J]. Materials Characterization, 2020, 167: 110489.

[16] Mao S L, Zhang D Z, Ren Z H, et al. Effects of process parameters on interfacial characterization and mechanical properties of 316L/CuCrZr functionally graded material by selective laser melting[J]. Journal of Alloys and Compounds, 2022, 899: 163256.

[17] Erinosho M F, Akinlabi E T, Pityana S. Effect of scanning speed and powder flow rate on the evolving properties of laser metal deposited Ti-6Al-4V/Cu composites[J]. International Journal of Surface Science and Engineering, 2016, 10(3): 207-223.

[18] Marques A, Cunha A, Gasik M, et al. 3D multi-material laser powder bed fusion: Ti6Al4V-CuNi2SiCr parts for aerospace applications[J]. Progress in Additive Manufacturing, 2023: 1-20.

[19] Wei C, Liu L C, Cao H T, et al. Cu10Sn to Ti6Al4V bonding mechanisms in laser-based powder bed fusion multiple material additive manufacturing with different build strategies[J]. Additive Manufacturing, 2022, 51: 102588.

[20] Sing S L, Lam L P, Zhang D Q, et al. Interfacial characterization of SLM parts in multi-material processing: Intermetallic phase formation between AlSi10Mg and C18400 copper alloy[J]. Materials Characterization, 2015, 107: 220-227.

[21] Su Y, Chen B, Tan C W, et al. Influence of composition gradient variation on the microstructure and mechanical properties of 316 L/Inconel718 functionally graded material fabricated by laser additive manufacturing[J]. Journal of Materials Processing Technology, 2020, 283: 116702.

[22] 余满江, 吴成萌, 冯爱新, 等. 激光沉积制备316L-IN625梯度材料的组织与力学性能[J]. 中国激光, 2022, 49(8): 0802007.
Yu M J, Wu C M, Feng A X, et al. Microstructure and mechanical properties of 316L-IN625 gradient material prepared via laser deposition[J]. Chinese Journal of Lasers, 2022, 49(8): 0802007.

[23] Aydogan B, O'Neil A, Sahasrabudhe H. Microstructural and mechanical characterization of stainless steel 420 and Inconel 718 multi-material structures fabricated using laser directed energy deposition[J]. Journal of Manufacturing Processes, 2021, 68: 1224-1235.

[24] 黄金鑫, 孙中刚, 常辉, 等. 激光增材制造Ti6Al4V-Inconel718功能梯度材料的成分变化和微观结构演变[J]. 稀有金属材料与工程, 2020, 49(8): 2813-2819.
Huang J X, Sun Z G, Chang H, et al. Compositional changes and microstructure evolution of Ti6Al4V-Inconel718 functionally graded materials by laser additive manufacturing[J]. Rare Metal Materials and Engineering, 2020, 49(8): 2813-2819.

[25] Zhang C, Chen F, Wang Q, et al. Additive manufacturing and mechanical properties of TC4/Inconel 625 functionally graded materials by laser engineered net shaping[J]. Materials Science and Engineering: A, 2023, 862: 144370.

[26] Bartolomeu F, Costa M M, Alves N, et al. Additive manufacturing of NiTi-Ti6Al4V multi-material cellular structures targeting orthopedic implants[J]. Optics and Lasers in Engineering, 2020, 134: 106208.

[27] Su Y Y, Wang Z F, Xie J C, et al. Microstructures and mechanical properties of laser melting deposited Ti6Al4V/316L functional gradient materials[J]. Materials Science and Engineering: A, 2021, 817: 141355.

[28] Miao H, Yusof F, Ab Karim M S, et al. Interfacial microstructure, element diffusion, mechanical properties and metallurgical bonding mechanism of 316L-AlSi10Mg multi-material parts fabricated by laser powder bed fusion[J]. Journal of Materials Research and Technology, 2023, 26: 8351-8365.

[29] Nguyen D S, Park H S, Lee C M. Applying selective laser melting to join Al and Fe: an investigation of dissimilar materials[J]. Applied Sciences, 2019, 9(15): 3031.

[30] Wu X P, Zhang D Y, Yi D H, et al. Interfacial characterization and reaction mechanism of Ti/Al multi-material structure during laser powder bed fusion process[J]. Materials Characterization, 2022, 192: 112195.

[31] Zhang D Q, Du D, Pu Z, et al. Interfacial microstructure and stress characteristics of laser-directed energy deposited AA2024 on Ti6Al4V substrate[J]. Optics Laser Technology, 2023, 164: 109521.

[32] Zhang Y N, Bandyopadhyay A. Direct fabrication of bimetallic Ti6Al4V+Al12Si structures via additive manufacturing[J]. Additive Manufacturing, 2019, 29: 100783.

[33] Bartolomeu F, Carvalho O, Gasik M, et al. Multi-functional Ti6Al4V-CoCrMo implants fabricated by multi-material laser powder bed fusion technology: a disruptive material's design and manufacturing philosophy[J]. Journal of the Mechanical Behavior of Biomedical Materials, 2023, 138: 105583.

[34] Wen Y J, Zhang B C, Narayan R L, et al. Laser powder bed fusion of compositionally graded CoCrMo-Inconel 718[J]. Additive Manufacturing, 2021, 40: 101926.

[35] Yao L M, Ramesh A, Fan Z H, et al. Interface analysis between Inconel 625 and cobalt-chromium alloy fabricated by powder bed fusion using pulsed wave laser[J]. Materials, 2023, 16(19): 6456.

[36] Reddy Y P, Narayana K L, Mallik M K, et al. Experimental evaluation of additively deposited functionally graded material samples-microscopic and spectroscopic analysis of SS-316L/Co-Cr-Mo alloy[J]. AIMS Materials Science, 2022, 9(4): 653-667.

[37] Wei C, Liu L C, Gu Y C, et al. Multi-material additive-manufacturing of tungsten - copper alloy bimetallic structure with a stainless-steel interlayer and associated bonding mechanisms[J]. Additive Manufacturing, 2022, 50: 102574.

[38] Zhou Y, Duan L C, Li F, et al. Effect of heat treatment on the microstructure and mechanical property of W/316L multi-material fabricated by selective laser melting[J]. Journal of Alloys and Compounds, 2022, 890: 161841.

[39] Gradl P R, Teasley T W, Protz C S, et al. Advancing GRCop-based bimetallic additive manufacturing to optimize component design and applications for liquid rocket engines[C]//Proceedings of the AIAA Propulsion and Energy 2021 Forum, August 9-11, 2021, Virtual event. Virginia: AIAA Press, 2021: 3231.

[40] Gradl P R, Protz C, Fikes J, et al. Lightweight Thrust Chamber Assemblies using Multi-Alloy Additive Manufacturing and Composite Overwrap[C]//Proceedings of the AIAA Propulsion and Energy 2020 Forum, August 24-28, 2020, Virtual event. Virginia: AIAA Press, 2020: 3787.

[41] 3D科学谷. (一)金属与金属|多材料和蜂窝超材料的3D打印设计、特性、应用、挑战[EB/OL]. (2023-04-17)[2023-12-27]. https://mp.weixin.qq.com/s/AlDpfRlU53jBt0AgTZpSQQ.
3DScience ValleyD. Design, characteristics, applications, and challenges of 3D printing for metal and metal multimaterials and honeycomb metamaterials[EB/OL]. (2023-04-17) [2023-12-27]. https://mp.weixin.qq.com/s/AlDpfRlU53jBt0AgTZpSQQ.

[42] AMLetters. Fraunhofer联合SLM Solutions突破多材料金属打印[EB/OL]. (2022-07-23)[2023-12-27]. https://mp.weixin.qq.com/s/P5NrRBBZuYp4FUPVLJaryg.
AMLetters. Fraunhofer collaborates with SLM Solutions to break through multi material metal printing[EB/OL]. (2022-07-23)[2023-12-27]. https://mp.weixin.qq.com/s/P5NrRBBZuYp4FUPVLJaryg.

[43] Schneck M, Horn M, Schindler M, et al. Capability of multi-

material laser-based powder bed fusion: development and analysis of a prototype large bore engine component[J]. Metals, 2021, 12(1): 44.
[44] 深圳国际增材制造与粉末冶金展.【快讯・工艺】Formnext2022上悄然兴起的金属多材料增材制造以及混合制造技术[EB/OL]. (2022-12-14) [2023-12-28]. https://mp.weixin.qq.com/s/4BRSXMciVdkZsQdC35MZBA.
Shenzhen International Additive Manufacturing and Powder Metallurgy Exhibition. [Quick News · Craftsmanship] The quietly emerging metal multi material additive manufacturing and hybrid manufacturing technology on Formnext2022[EB/OL]. (2022-12-14) [2023-12-28]. https://mp.weixin.qq.com/s/4BRSXMciVdkZsQdC35MZBA.
[45] Wits W W, Amsterdam E. Graded structures by multi-material mixing in laser powder bed fusion[J]. CIRP Annals, 2021, 70(1): 159-162.
[46] Aerosint. Printing services[EB/OL]. (2020-12-17) [2023-12-27]. https://aerosint.com/printing-services/.
[47] Hofmann D C, Kolodziejska J, Roberts S, et al. Compositionally graded metals: a new frontier of additive manufacturing[J]. Journal of Materials Research, 2014, 29(17): 1899-1910.
[48] Admin. 探秘国产增减混合五轴加工中心[EB/OL]. (2017-02-28) [2023-12-27]. https://www.3ddayin.net/news/guonadongtai/28627.html.
Admin. Exploring the domestic addition and reduction hybrid five axis machining center[EB/OL]. (2017-02-28)[2023-12-27]. https://www.3ddayin.net/news/guonadongtai/28627.html.
[49] Domack M S, Baughman J M. Development of nickel-titanium graded composition components[J]. Rapid Prototyping Journal, 2005, 11(1): 41-51.
[50] Wei C, Li L. Recent progress and scientific challenges in multi-material additive manufacturing via laser-based powder bed fusion[J]. Virtual and Physical Prototyping, 2021, 16(3): 347-371.
[51] 韦超, 杨潇, 鲁淑芬, 等. 激光多材料增材制造技术研究进展和展望[J]. 航空制造技术, 2023, 66(8): 26-34.
Wei C, Yang X, Lu S F, et al. Research progress and prospect of laser-based multi-material additive manufacturing technology[J]. Aeronautical Manufacturing Technology, 2023, 66(8): 26-34.
[52] Tian X X, Zhao Z, Wang H B, et al. Progresses on the additive manufacturing of functionally graded metallic materials[J]. Journal of Alloys and Compounds, 2023, 960: 170687.
[53] Zhang C, Chen F, Huang Z F, et al. Additive manufacturing of functionally graded materials: a review[J]. Materials Science and Engineering: A, 2019, 764: 138209.
[54] Bandyopadhyay A, Heer B. Additive manufacturing of multi-material structures[J]. Materials Science and Engineering: Reports, 2018, 129: 1-16.
[55] 张百成, 王泳翔, 曲选辉. 基于增材制造的异种金属一体化成形关键问题[J]. 航空制造技术, 2023, 66(18): 36-50.
Zhang B C, Wang Y X, Qu X H. Key issues of integrated forming of dissimilar metals based on additive manufacturing[J]. Aeronautical Manufacturing Technology, 2023, 66(18): 36-50.
[56] Yao J, Xin B, Gong Y D, et al. Effect of initial temperature on the microstructure and properties of stellite-6/Inconel 718 functional gradient materials formed by laser metal deposition[J]. Materials, 2021, 14(13): 3609.
[57] Ostolaza M, Arrizubieta J I, Lamikiz A, et al. Functionally graded AISI 316L and AISI H13 manufactured by L-DED for die and mould applications[J]. Applied Sciences, 2021, 11(2): 771. [LinkOut]
[58] MORIDMG. LASERTEC 6600[EB/OL]. [2023-12-28]. https://cn.dmgmori.com.cn/products/machines/additive-manufacturing/powder-nozzle/lasertec-6600-ded-hybrid.
[59] Chen J P, Xie S C, Huang H. A novel method of utilizing static mixer to obtain mixing homogeneity of multi-species powders in laser metal deposition[J]. Chinese Journal of Aeronautics, 2023, 36(1): 423-433.
[60] Daram P, Hiroto T, Watanabe M. Microstructure and phase evolution of functionally graded multi-materials of Ni-Ti alloy fabricated by laser powder bed fusion process[J]. Journal of Materials Research and Technology, 2023, 23: 5559-5572.
[61] Errico V, Posa P, Fusco A, et al. Intralayer multi-material structure stainless-steel/nickel-superalloy fabricated via laser-powder bed fusion process[J]. Manufacturing Letters, 2023, 35: 11-15.
[62] Al-Jamal O M, Hinduja S, Li L. Characteristics of the bond in Cu-H13 tool steel parts fabricated using SLM[J]. CIRP Annals, 2008, 57(1): 239-242.
[63] Wei C, Zhang Z Z, Cheng D X, et al. An overview of laser-based multiple metallic material additive manufacturing: from macro- to micro-scales[J]. International Journal of Extreme Manufacturing, 2021, 3(1): 012003.
[64] Aerosint. Multi-material L-PBF [EB/OL]. (2022-04-26)[2024-01-24]. https://aerosint.com/multi-material-3d-printing-bundle/.
[65] Wei C, Gu H, Gu Y C, et al. Abnormal interfacial bonding mechanisms of multi-material additive-manufactured tungsten-stainless steel sandwich structure[J]. International Journal of Extreme Manufacturing, 2022, 4(2): 025002.
[66] Wei C, Sun Z, Chen Q, et al. Additive manufacturing of horizontal and 3D functionally graded 316L/Cu10Sn components via multiple material selective laser melting[J]. Journal of Manufacturing Science and Engineering, 2019, 141(8): 081014.
[67] Errico V, Posa P, Liang L, et al. Layer-level AISI 316L-18Ni (300) Maraging multi-material fabrication via Laser-Powder Bed Fusion[J]. Materials Science and Engineering: A, 2023, 886: 145731.
[68] Yoo S W, Lee C M, Kim D H. Effect of functionally graded material (FGM) interlayer in metal additive manufacturing of inconel-stainless bimetallic structure by laser melting deposition (LMD) and wire arc additive manufacturing (WAAM)[J]. Materials, 2023, 16(2): 535.
[69] Ozsoy A, Tureyen E B, Baskan M, et al. Microstructure and mechanical properties of hybrid additive manufactured dissimilar 17-4 PH and 316L stainless steels[J]. Materials Today Communications, 2021, 28: 102561.
[70] Zhang B P, Zhang W Q, Xiao H F, et al. $QCr_{0.8}$ Cu alloy/S06 stainless steel bimetal structure via In718 multi-interlayer fabricated by laser powder hybrid additive manufacturing[J]. Journal of Materials Research and Technology, 2023, 24: 1034-1042.
[71] Rodrigues J P, Thanumoorthy R S, Manjhi S K, et al. Hybrid additive manufacturing of ER70S6 steel and Inconel 625: a study on microstructure and mechanical properties[J]. Materials Today Communications, 2023, 37: 106977.
[72] Bettencourt C J, Kouraytem N. Microstructural characterization of the transition in SS316L and IN625 bimetallic fabricated using hybrid additive manufacturing[J]. JOM, 2023, 75(12): 5079-5087.
[73] Yin S, Yan X C, Chen C Y, et al. Hybrid additive manufacturing of Al-Ti6Al4V functionally graded materials with selective laser melting and cold spraying[J]. Journal of Materials Processing Technology, 2018, 255: 650-655.
[74] Liu L Q, Wang D, Deng G W, et al. Laser additive manufacturing of a 316L/CuSn10 multimaterial coaxial nozzle to alleviate spattering adhesion and burning effect in directed energy deposition[J]. Journal of Manufacturing Processes, 2022, 82: 51-63.
[75] Kuai Z Z, Li Z H, Liu B, et al. Microstructure and mechanical properties of CuCrZr/316L hybrid components manufactured using selective laser melting[J]. Journal of Alloys and Compounds, 2023, 955: 170103.
[76] Liu S, Liu C S, Yuan C. Process parameter optimization for the laser metal deposition of a functionally graded GH4169/K417G superalloy and the effects of preheating and composition on cracking behavior[J]. Journal of Materials Engineering and Performance, 2023: 1-17.
[77] Bandyopadhyay A, Zhang Y N, Onuike B. Additive

manufacturing of bimetallic structures[J]. Virtual and Physical Prototyping, 2022, 17(2): 256-294.

[78] Zhang C, Liu Y, Lu J Q, et al. Additive manufacturing and mechanical properties of martensite/austenite functionally graded materials by laser engineered net shaping[J]. Journal of Materials Research and Technology, 2022, 17: 1570-1581.

[79] Tey C F, Tan X P, Sing S L, et al. Additive manufacturing of multiple materials by selective laser melting: Ti-alloy to stainless steel via a Cu-alloy interlayer[J]. Additive Manufacturing, 2020, 31: 100970.

[80] Onuike B, Bandyopadhyay A. Additive manufacturing of Inconel 718-Ti6Al4V bimetallic structures[J]. Additive Manufacturing, 2018, 22: 844-851.

[81] Wei C, Li L, Zhang X J, et al. 3D printing of multiple metallic materials via modified selective laser melting[J]. CIRP Annals, 2018, 67(1): 245-248.

[82] Li X R, Li Q, Nie M H, et al. Evading the strength-ductility trade-off dilemma in steel-nickel heterostructured material by bionic crossed-lamellar structures[J]. Virtual and Physical Prototyping, 2023, 18(1): 2266640.

[83] Li L, Zhang X C, Cui W Y, et al. Temperature and residual stress distribution of FGM parts by DED process: modeling and experimental validation[J]. The International Journal of Advanced Manufacturing Technology, 2020, 109(1): 451-462.

[84] Ghanavati R, Lannunziata E, Norouzi E, et al. Design and development of SS316L-IN718 functionally graded materials via laser powder bed fusion[J]. Materials Letters, 2023, 349: 134793.

[85] Demir A G, Kim J, Caltanissetta F, et al. Enabling multi-material gradient structure in laser powder bed fusion[J]. Journal of Materials Processing Technology, 2022, 301: 117439.

[86] 李星燃, 刘政麟, 姜鹏飞, 等. 激光增材制造Ti6Al4V/NiTi仿生功能梯度材料的界面特征及性能[J]. 焊接学报, 2023, 44(10): 27-33.
Li X R, Liu Z L, Jiang P F, et al. Interface characteristics and properties of Ti6Al4V/NiTi biomimetic functionally graded materials manufactured by laser additive[J]. Transactions of the China Welding Institution, 2023, 44(10): 27-33.

[87] 王辰阳, 邢飞, 刘祥宇, 等. Cu过渡层对直接激光沉积TC4/IN718双金属结构组织性能的影响[J]. 稀有金属材料与工程, 2023, 52(1): 323-31.
Wang C Y, Xing F, Liu X Y, et al. Effect of Cu interlayer on microstructure and properties of TC4/IN718 bimetallic structure fabricated by directed laser deposition[J]. Rare Metal Materials and Engineering, 2023, 52(1): 323-331.

[88] 王文博, 徐诺, 徐国建, 等. Cu夹层激光熔化沉积IN625/TC4双金属结构过渡区组织与性能的研究[J]. 钢铁钒钛, 2023, 44(4): 48-54.
Wang W B, Xu N, Xu G J, et al. Study on the microstructure and properties of the transition region of IN625/TC4 bimetallic structure by laser melting deposition with Cu interlayer[J]. Iron Steel Vanadium Titanium, 2023, 44(4): 48-54.

[89] Zhang J L, Wang X B, Gao J B, et al. Additive manufacturing of Ti-6Al-4V/Al-Cu-Mg multi-material structures with a Cu interlayer[J]. International Journal of Mechanical Sciences, 2023, 256: 108477.

[90] Wang C D, Zhang P Q, Zhang K D, et al. A novel process parameter screening strategy by comprehensively consideration of powder separation, defects and power consumption when fabricating FGM using laser metal deposition[J]. Journal of Cleaner Production, 2021, 278: 123274.

[91] Sun Z G, Ji X, Zhang W S, et al. Microstructure evolution and high temperature resistance of Ti6Al4V/Inconel625 gradient coating fabricated by laser melting deposition[J]. Materials & Design, 2020, 191: 108644.

[92] Ma R X, Liu Z Q, Wang W B, et al. Microstructures and mechanical properties of Ti6Al4V-Ti48Al2Cr2Nb alloys fabricated by laser melting deposition of powder mixtures[J]. Materials Characterization, 2020, 164: 110321.

[93] Scaramuccia M G, Demir A G, Caprio L, et al. Development of processing strategies for multigraded selective laser melting of Ti_6Al_4V and IN718[J]. Powder Technology, 2020, 367: 376-389.

[94] Fan H Y, Shi Q M, Wang C C, et al. Laser powder bed fusion of bimetallic stainless steel/Nickel-based superalloy: interface and mechanical properties[J]. Materials Science and Engineering: A, 2023, 877: 145193.

[95] 李鹏飞, 李亮亮, 周建忠, 等. 激光增材制造不同成分变化率316L/IN718功能梯度材料组织性能研究[J]. 机械工程学报, 2022, 58(17): 226-39.
Li P F, Li L L, Zhou J Z, et al. Microstructure and properties of 316L/IN718 functionally graded materials with different composition gradients fabricated by laser additive manufacturing[J]. Journal of Mechanical Engineering, 2022, 58(17): 226-39.

[96] 张超, 吴定勇, 杨辉, 等. 激光熔化沉积制备316L/TC4梯度材料微观组织及力学性能[J]. 焊接技术, 2022, 51(11): 1-6, 113.
Zhang C, Wu D Y, Yang H, et al. Microstructure and mechanical properties of 316L/TC4 gradient materials prepared by laser melting deposition[J]. Welding Technology, 2022, 51(11): 1-6, 113.

[97] Yusuf S M, Zhao X, Yang S F, et al. Interfacial characterisation of multi-material 316L stainless steel/Inconel 718 fabricated by laser powder bed fusion[J]. Materials Letters, 2021, 284: 128928.

[98] Tong X Y, Lu C X, Huang Z F, et al. Microstructures and mechanical properties of crack-free 316L stainless steel and Inconel 625 joint by using Laser Engineered Net Shaping[J]. Optics Laser Technology, 2022, 155: 108357. [LinkOut]

[99] Prasad H S, Brueckner F, Volpp J, et al. Laser metal deposition of copper on diverse metals using green laser sources[J]. The International Journal of Advanced Manufacturing Technology, 2020, 107(3): 1559-1568.

[100] Wasmer K, Wüst M, Cui D, et al. Monitoring of functionally graded material during laser directed energy deposition by acoustic emission and optical emission spectroscopy using artificial intelligence[J]. Virtual and Physical Prototyping, 2023, 18(1): 2189599.

[101] Chen W Y, Zhang X, Li M M, et al. Laser powder bed fusion of Inconel 718 on 316 stainless steel[J]. Additive Manufacturing, 2020, 36: 101500.

[102] Chen B, Meng Z, Yang K, et al. A study on the relationship between spectral characterization and composition of plasma in laser additive manufacturing of gradient materials[J]. Rapid Prototyping Journal, 2022, 28(4): 756-765.

[103] Kumar B, Jaya B N. Thermal stability and residual stresses in additively manufactured single and multi-material systems[J]. Metallurgical and Materials Transactions A, 2023, 54(5): 1808-1824.

[104] Miao H, Yusof F, Karim M S A, et al. Process parameter optimisation for selective laser melting of AlSi10Mg-316L multi-materials using machine learning method[J]. The International Journal of Advanced Manufacturing Technology, 2023, 129(7): 3093-3108.

[105] Sun Z, Chueh Y H, Li L. Multiphase mesoscopic simulation of multiple and functionally gradient materials laser powder bed fusion additive manufacturing processes[J]. Additive Manufacturing, 2020, 35: 101448.

[106] 张昊, 戴冬华, 石新宇, 等. 激光直接能量沉积316L/Inconel 718多材料熔池热行为[J]. 中国激光, 2022, 49(14): 1402208.
Zhang H, Dai D H, Shi X Y, et al. Thermal behavior of molten pool for laser directed energy deposition of 316L/Inconel 718 multi-materials[J]. Chinese Journal of Lasers, 2022, 49(14): 1402208.

[107] 孙成, 孙亦璋, 刘金, 等. 激光增材制造TC4/TC11钛合金梯度结构温度场预测与显微组织分析[J]. 航空制造技术, 2018, 61(4): 96-101.
Sun C, Sun Y Z, Liu J, et al. Temperature field prediction and microstructure analysis of gradient TC4/TC11 titanium alloy

deposited by laser additive manufacturing[J]. Aeronautical Manufacturing Technology, 2018, 61(4): 96-101.
[108] Yan J Y, Battiato I, Fadel G M. Planning the process parameters for the direct metal deposition of functionally graded parts based on mathematical models[J]. Journal of Manufacturing Processes, 2018, 31: 56-71.
[109] Rankouhi B, Jahani S, Pfefferkorn F E, et al. Compositional grading of a 316L-Cu multi-material part using machine learning for the determination of selective laser melting process parameters[J]. Additive Manufacturing, 2021, 38: 101836.
[110] Wei M, Yin X H, Wang Z, et al. Additive manufacturing of a functionally graded material from Inconel625 to Ti6Al4V by laser synchronous preheating[J]. Journal of Materials Processing Technology, 2020, 275: 116368.
[111] Pellizzari M, Zhao Z, Bosetti P, et al. Optimizing direct laser metal deposition of H13 cladding on CuBe alloy substrate[J]. Surface and Coatings Technology, 2022, 432: 128084.
[112] Wen Y J, Gao J B, Narayan R L, et al. Microstructure-property correlations in as-built and heat-treated compositionally graded stainless steel 316L-Inconel 718 alloy fabricated by laser powder bed fusion[J]. Materials Science and Engineering: A, 2023, 862: 144515.
[113] Pasco J, Tian Y, Chadha K, et al. Unusual interface phase transformation during continuous additive manufacturing of maraging steel and Co-30Cr-7Mo alloy[J]. Materials Science and Engineering: A, 2023, 881: 145336.
[114] Borisov E, Polozov I, Starikov K, et al. Structure and properties of Ti/Ti64 graded material manufactured by laser powder bed fusion[J]. Materials, 2021, 14(20): 6140.
[115] 吴润宝, 徐刚, 罗开玉, 等. 热处理对激光增材 In718/316L 功能梯度材料组织和性能的影响[J]. 机械工程学报, 2022, 58(19): 293-305.
Wu R B, Xu G, Luo K Y, et al. Effects of heat treatment on microstructure and tensile properties of laser additive manufactured In718/316L functionally gradient material[J]. Journal of Mechanical Engineering, 2022, 58(19): 293-305.

Research and Application Progress in Laser Additive Manufacturing of Heterogeneous Metals (Invited)

Ma Yi[1], Guan Yingchun[1,2*]

[1]*School of Mechanical Engineering and Automation, Beihang University, Beijing* 100083, *China*;
[2]*National Engineering Laboratory of Additive Manufacturing for Large Metallic Components, Beihang University, Beijing* 100191, *China*

Abstract

Significance Major advances in materials science and manufacturing technology are being driven by fields such as aerospace, which are placing increasingly stringent requirements for the construction of complex, reliable, and high-performance components intended for extreme service conditions. For example, engine components must possess both high heat resistance and excellent thermal conductivity, while structural component aim with a combination of lightweight design and high strength. These intricate performance demands have spurred the development of heterogeneous metal integration, wherein different materials with complementary properties are integrated into a single component through optimized design and manufacturing process control. This approach aims to break through the performance limits of traditional single-material components and broaden their application scenarios. The effective connection between heterogeneous metals has always been a major challenge in the engineering field. Because of the inherent differences in the physicochemical properties of various metals, achieving a high-strength and reliable interface bonding through traditional welding or mechanical connection methods is often challenging. This difficulty is particularly pronounced when dealing with complex interface shapes or gradient functional areas. However, laser additive manufacturing technology, owing to its high forming precision and controllability, has provided a novel pathway for heterogeneous metal manufacturing. This technology significantly enhances the freedom of material design and shaping, enabling reliable connections between heterogeneous metals. Laser additive technology primarily includes laser powder bed fusion (LPBF) and laser directed energy deposition (LDED). These technologies can respectively meet the manufacturing needs of complex or large heterogeneous aerospace components. LPBF produces parts with a high degree of surface finish and intricate structures by preforming layers of dissimilar powders and selectively melting them layer by layer. In contrast, LDED uses lasers to deposit powder or wire materials onto a substrate and provides high flexibility and freedom in manufacturing. However, the maturity of both LPBF and LDED technologies is not yet sufficiently high, and they face various issues in practical applications. Therefore, it is imperative to systematically summarize and discuss existing research to facilitate the rapid development of this field.

Progress The development of laser additive manufacturing technology has expanded the variety of heterogeneous metal connections, enabling performance customization according to the demands of various application scenarios, such as in the aerospace, medical, automotive, and petrochemical industries (Table 1). In the aerospace field, heterogeneous metals like Cu/Ni, Fe-based, and Ti-based alloys can be utilized for manufacturing power components and load-bearing structural components (Figs. 1–3) to meet the requirements of work in extreme environments. However, traditional laser additive manufacturing equipment poses several limitations in the preparation of heterogeneous metals (Table 2). For example, it faces challenges in achieving precise powder delivery and deposition, as well as limitations in the connection of heterogeneous composition within layers. Therefore, improvements are required in powder delivery, blending, and processing devices (Figs. 4–5). Additionally, the integration of additive manufacturing

methods (Fig. 6) can enhance the forming efficiency and quality of heterogeneous metals. For heterogeneous metal components, interface quality is of utmost importance and is primarily determined by the physicochemical properties of heterogeneous alloys and processing parameters (Fig. 7). The complex physicochemical differences among heterogeneous metals, such as differences in thermal expansion coefficients, melting points, density, surface tension, elastic modulus, and mismatched crystal structures, along with variations in their response to laser processing, can lead to a range of macroscopic and microscopic defects. These defects include voids, cracks, harmful phases (brittle intermetallic compounds, oxide inclusions), and residual stresses, which significantly impact the interface quality and forming effectiveness. To avoid defects during the manufacturing process, it is critical to enhance the bonding quality between heterogeneous metals, optimize connection methods (Fig. 8), and control process parameters (Fig. 9). This involves achieving reliable connections between materials with disparate properties using gradient layers/intermediate layers and adjusting the laser parameters to match the bonding process of heterogeneous metals. Furthermore, employing online monitoring (Fig. 10) and intelligent prediction methods (Fig. 11) during the manufacturing process can enable efficient process control, thus reducing trial-and-error costs and significantly improving the efficiency of heterogeneous metal connections. Simultaneously, pre-processing (Fig. 12) and post-processing (Fig. 13) can optimize the organization and performance of heterogeneous metal interfaces, improving the quality of the formed components.

Conclusions and Prospects Heterogeneous metal laser additive manufacturing technology has significant advantages in realizing functional integration and reliable manufacturing of complex components. This paper provides a comprehensive overview of the material systems, relevant applications, equipment development, and process optimization in the field of laser additive manufacturing of heterogeneous metals. The article discusses restrictive issues encountered during the additive manufacturing of heterogeneous metals, including limitations in manufacturing equipment, material incompatibility, and mismatched process parameters. It also summarizes and outlines the corresponding solutions, encompassing optimized connection strategies and processing parameters, the use of monitoring and prediction methods, as well as efficient pre-processing and post-processing techniques. Despite facing several challenges, the continuous development of related equipment and processes suggests that this technology will better serve industries such as aerospace in the future.

Key words laser technique; heterogeneous metal; aerospace applications; additive manufacturing equipment; additive manufacturing technique